CHALMERS
UNIVERSITY OF TECHNOLOGY

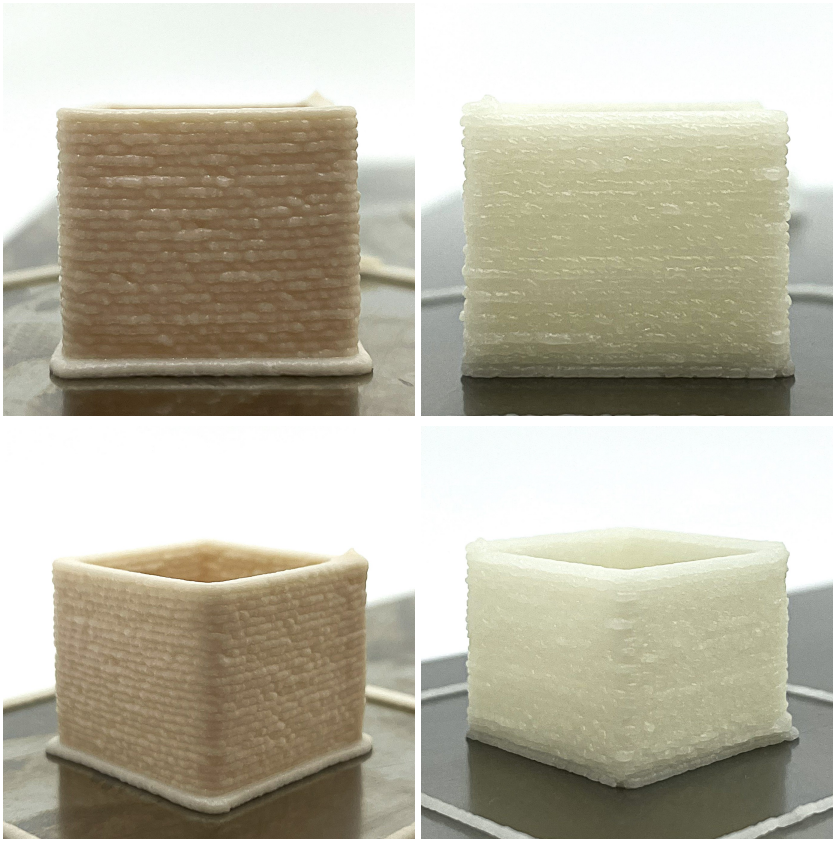

Evaluation of emulsion gels and bigels as animal fat substitutes in multi-material food 3D printing

Investigation of dual and coaxial extrusion techniques and rheological properties for functional fat replacement

Master's Thesis in Biotechnology, Food and Nutrition Science

Linnea Johansson

DEPARTMENT OF LIFE SCIENCES

CHALMERS UNIVERSITY OF TECHNOLOGY
Gothenburg, Sweden 2025
www.chalmers.se

Master's thesis 2025

Evaluation of emulsion gels and bigels as animal fat substitutes in multi-material food 3D printing

Investigation of dual and coaxial extrusion techniques and rheological properties for functional fat replacement

LINNEA JOHANSSON

CHALMERS
UNIVERSITY OF TECHNOLOGY

Department of Life Sciences
Division of Food and Nutrition Science
Chalmers University of Technology
Gothenburg, Sweden 2025

Evaluation of bigels and emulsion gels as animal fat substitutes in multi-material food 3D printing
Investigation of dual and coaxial extrusion techniques and rheological properties for functional fat replacement
Linnea Johansson

Supervisor: Mikaela Isabel Badager, Food and Nutrition Science
Examiner: Mehdi Abdollahi, Food and Nutrition Science

Master's Thesis 2025
Department of Life Sciences
Division of Food and Nutrition Science
Chalmers University of Technology
SE-412 96 Gothenburg
Telephone +46 31 772 1000

Cover: Visual comparison of 3D printed structures made from emulsion gel (left) and bigel (right).

Typeset in LaTeX
Printed by Chalmers Reproservice
Gothenburg, Sweden 2025

Abstract

To successfully develop plant-based meat analogs, it is essential not only to mimic the protein content of conventional meat, but to also replicate the structural and functional roles of animal fat. This thesis investigates two approaches for structuring liquid oils, emulsion gels and bigels, for use as fat substitutes in food 3D printing.

The study was conducted in two phases. In the first, the rheological properties, printability in single material printing and microstructure of both gels were evaluated. The second investigated their performance in multi-material 3D printing when combined with a pea protein isolate-based ink, using dual and coaxial extrusion techniques.

Rheological analyses, including amplitude sweep, shear-viscosity test, frequency sweep, three interval thixotropy test and temperature sweep, revealed distinct differences in behaviours for each gel. The bigel showed higher initial viscosity and greater thermal sensitivity, but also stronger shear-thinning and self-supporting properties. The emulsion gel was softer and less structurally stable. Confocal laser scanning microscopy provided further insights into the gels' microstructure and phase distribution, supporting the rheological findings.

In 3D printing, both gels were printable using the same G-code with the same printing parameters. However, the bigel retained better definition and buildability, and could withstand increased layer heights, where emulsion gel collapsed. In multi-material 3D printing, the bigel maintained structural integrity when printed together with PPI30, in contrast to emulsion gel, which exhibited poor material distribution and inconsistent extrusion behaviour. The bigel also showed superior storage stability, maintaining their form over extended periods at room temperature.

The results demonstrate that while both gel systems are potential options for structured fat replacement, bigel offer greater mechanical stability and compatibility for use in food 3D printing. These findings contribute to the development of more realistic plant-based meat analogs and highlight the importance of optimizing both material formulation and printing techniques.

Acknowledgements

First of all, I would like to sincerely thank my examiner, Mehdi Abdollahi, for giving me the opportunity to carry out my thesis within his research group and for his valuable feedback and support throughout the project, and especially for believing in and encouraging me!

A special thanks goes to my supervisor, Mikaela Isabel Badager, for her dedicated guidance and for always taking the time to help. Her expertise and support have been invaluable to both the process and the outcome of this work.

I would also like to thank my colleagues in the FNS division for warmly welcoming me into the group and for creating such a supportive and positive environment. Your help and the friendly atmosphere have made this experience both productive and enjoyable.

Finally, I am deeply grateful to my family and friends for always cheering me on and supporting me throughout this journey.

List of abbreviations

3DP	3D printing
CLSM	Confocal laser scanning microscopy
LVE	Linear viscoelastic region
MM3DP	Multi-material 3D printing
MUFA	Monounsaturated fatty acid
O/W	Oil-in-water
PPI	Pea protein isolate
PPI30	Pea protein isolate at 30 wt%
PUFA	Polyunsaturated fatty acid
SFA	Saturated fatty acid
TFA	Trans fatty acid
UFA	Unsaturated fatty acid
W/O	Water-in-oil

Table of contents

1 Introduction

As the awareness of environmental, ethical and health-related concerns regarding animal-derived food products increases, the demand for plant-based alternatives simultaneously continues to grow. In the development of these food items, much of the focus has previously been on protein content, while fats have not received the same attention [1]. This despite their great contribution in the overall sensation of plant-based meat analogs, particularly in texture, mouthfeel and flavour [2].

A key challenge in replacing animal fats is replicating their functional properties as they remain solid at room temperature, whereas plant-based oils typically are liquid [2]. To address this issue, methods for structuring the liquid oils into more solid-like fats are required. One promising strategy involves the use of gel systems.

Gels are three-dimensional networks, primarily composed of two components: a liquid medium and a dispersed solid network, which provide structural integrity and stability [3]. Among the available gel systems, two are of particular interest: emulsion gels and bigels.

In emulsion gels, an emulsion is embedded in a gel network [4]. Bigels, in contrast, are biphasic systems of two immiscible gel phases, typically a hydrogel and an oleogel [3]. Depending on their formulation, both gels can be of either water-in-oil (W/O) or oil-in-water (O/W) structure. While both systems have been explored in food applications, the comparison between the two in the context of food 3D printing (3DP) remains unexplored.

Food 3DP is an emerging technology that allows for precise deposition and customizable food materials, offering the possibility of creating plant-based meat analogs with complex structures [2]. Marbling is a key characteristic of meat, that refers to the distribution of intramuscular fat within muscle tissue that contributes to the juiciness, tenderness and flavor of meat, and replicating this structure is a major challenge [5].

Multi-material 3D printing (MM3DP) offers a potential solution to this issue, as it enables two materials to be extruded simultaneously, such as structured fats and

protein matrices [6]. The extrusion technique used in MM3DP plays a critical role in achieving complexity of the extruded objects. The two methods explored in this study are dual and coaxial extrusion. In dual extrusion, two materials are printed side by side while coaxial extrusion prints one material as the core and the other as a surrounding outer shell. These techniques offer approaches to improve the design of plant-based analogs.

The success of emulsion gels and bigels in 3DP depends on several factors, including their rheological properties, extrusion performance and compatibility with a second material in MM3DP. Understanding how these gels perform under different extrusion conditions is essential for optimizing their functionality as plant-based fat analogs.

This study aims to compare emulsion gels and bigels in MM3DP applications, evaluating their printability, structural stability and suitability as plant-based fat analogs in food 3DP products together with a pea protein isolate based ink.

1.1 Aim

The project aims to evaluate two gel systems, emulsion gel and bigel, and their suitability as animal fat analogs in food MM3DP. Additionally, two MM3DP extrusion techniques, dual and coaxial, are investigated.

This is further divided into the following specific aims:

- To evaluate and compare the suitability of emulsion gels and bigels for use in food 3DP as animal fat substitutes
- To evaluate and compare the suitability of emulsion gels and bigels for use in food MM3DP in combination with a pea protein isolate-based food ink
- To determine the optimal extrusion technique for food MM3DP, combining the pea protein isolate-based food ink with the gels respectively

To address these aims, the following research questions are investigated:

- What are the differences between emulsion gel and bigel food inks in terms of printability, rheological properties and microstructure?
- Which gel is most suitable for food MM3DP in combination with a pea protein

isolate-based ink?

- Which extrusion technique, dual or coaxial, is favourable for successful printing?

1.2 Specification of the issue being investigated

The development of plant-based fat analogs that can replace animal fats in food remains challenging primarily due to differences in physical and functional properties. Unlike animal fats, which are solid at room temperature, plant-based oils are liquid, which affects their texture and stability.

Previous studies have shown that bigels and emulsion gels can improve the structure of plant-based oils as fat analogs, but little is known about their performance in food 3DP, particularly in the context of plant-based meat analogs where fat substitutes should function together with other components. To the best of current knowledge, no studies have systematically evaluated their performance side-by-side in this context.

This study aims to address this gap by conducting a comparative evaluation of emulsion gels and bigels as fat analogs in food MM3DP. Through analysis of rheological properties, printability and microstructure, the research aims to determine which one is most suitable for food 3DP. Additionally, the study also investigates dual and coaxial extrusion techniques in MM3DP, which can offer strategies for incorporating the structured fats into plant-based food 3DP products.

1.3 Limitations

Certain limitations must be acknowledged in this study. The evaluation methods in the project focused on rheological properties, printability, and microstructure, while other important factors such as sensory properties and nutritional composition were not investigated due to time constraints. The number and complexity of the 3DP objects were restricted, also due to the time frame. The same G-code was applied for both gels, even though tailoring the printing parameters to each material would have likely improved their performance, but the project duration did not allow for these changes.

Additionally, a prototype mixing module made of plastic was used in the 3DP process, which led to a temperature decrease during extrusion since plastic does not maintain heat effectively. The final mixing module is intended to be constructed of stainless steel, which is important as printing performance of some materials relies on stable extrusion temperatures.

2 Background

2.1 Drivers of a shift towards plant-based alternatives

The transition from animal-based products to plant-based substitutes is primarily driven by an increasing awareness of environmental sustainability, ethical considerations and human health concerns.

Production of meat, such as beef, lamb and pork, has a significant impact on the environment, contributing to deforestation, methane emissions from livestock and farming processes with high resource demands. For instance, beef production requires extensive land use, generates over 100 times more greenhouse gas (GHG) emissions than plant-based alternatives like peas, and releases high levels of eutrophying emissions [7]. By shifting to plant-based substitutes, these environmental impacts can be significantly reduced.

Animal welfare is also a key driver of the transition. Consumers are becoming more aware of these concerns which increases the demand for alternatives with ethical practices. According to People for the Ethical Treatment of Animals (PETA), large-scale livestock farming often involves overcrowding, restricted movement and conditions during slaughter that can lead to significant animal suffering throughout their lives [8].

Health considerations further support the shift from animal-based products, particularly regarding the consumption of animal fats, that naturally contain trans fats (TFA) and saturated fats (SFA). In a meta-analysis performed by the World Health Organization (WHO), both SFA and TFA were linked to an increased risk of coronary heart disease. While evidence on SFA remains inconclusive, research consistently links TFA, especially industrially produced types, to negative health effects.

By addressing these environmental, ethical and health concerns, plant-based alternatives offer a sustainable solution to the challenges associated with conventional animal-based food production.

2.2 Current challenges in the adoption of plant-based analogs

Although there are many reasons behind this necessary shift in diet, the adoption of plant-based alternatives comes with challenges. One of the most critical issues is in replacing animal fats as they play a huge role in food structure and mouthfeel [2]. They contribute to juiciness, tenderness and flavour release, while also enhancing texture and colour. Furthermore, fats are not commonly prioritized in discussions of sustainable food, despite the fact that 45% of dietary fats globally are of animal origin [1]. This could potentially be due to a misunderstanding of their critical role in human health and their impact in sensory perception of food.

Another major barrier in the implementation of plant-based food products is consumer acceptance. Meat has long been a fundamental part of human diets, offering a good source of proteins, a variety of fats, minerals and vitamins, despite the potential health risks [9]. Its strong traditional and cultural significance makes change difficult, leading to skepticism and an unwillingness to accept plant-based alternatives.

To address the negative attitude towards meat analogues and increase consumer acceptance, they must meet certain criteria. First, they should achieve a sensory and textural resemblance to the meat product they aim to mimic. Secondly, they should provide a similar nutritional profile, particularly in protein and lipid content [10]. One characteristic influencing the quality of meat is marbling, which describes the complex distribution of fat within the muscle tissue [5]. The degree of marbling affects the juiciness, tenderness and flavor, as well as the cooking behaviour of animal fat, which melts at high temperatures and solidifies as it cools. Food 3D printing is a promising approach to overcoming the challenge in replicating the complex structure of meat, aiding in consumer acceptance of plant-based analogs [11].

Replacing animal fats with plant-based alternatives is also associated with textural challenges, since plant-based oils often are liquid at room temperature causing them to separate from the rest of the food matrix, unlike animal fats that are solid [2]. To address this issue, one common approach is to blend liquid oils with solid fats [12][13]. However, since solid fats are saturated, their use has been limited due to potential negative health effects. Producing solid fat systems free from SFAs and

TFAs is therefore a major obstacle in the food industry [14]. This could be addressed by structuring the healthier unsaturated fats (UFA) into more solid forms without changing their chemical composition [13]. A promising approach is the formulation of gelled systems, which provide a more stable structure without the incorporation of unhealthy fats.

2.3 Fat

Fats are a type of lipid primarily composed of triacylglycerols (TAGs), which consist of three fatty acids, each composed of a hydrocarbon chain attached to a carboxyl group esterified to a glycerol molecule [2][15]. Fats are responsible for multiple essential functions in the human body, including energy storage, acting as structural units of cellular membranes, controlling cholesterol levels and aiding in absorption of fat-soluble vitamins [16][1]. Their physical state at room temperature, along with their naming, is determined by the chemical structure and composition: lipids that are solid at room temperature are typically referred to as fats, while those that are liquid are called oils [16].

2.3.1 Types of fat

As previously mentioned, there are three types of fats: saturated, unsaturated and trans fats [17]. These groups are determined by their chemical composition of their hydrocarbon chain. In SFAs, the carbon atoms are connected through single bonds and each carbon atom is thus saturated with hydrogen atoms. This composition results in linear chains which allow for a more compact structure, resulting in SFAs being solid at room temperature. Fats of animal origin, like butter or in red meat, usually contain high amounts of SFAs. They are also found in some vegetable oils, like palm and coconut oil.

UFAs have at least one double bond in the fatty acid chain [16]. These can be divided into mono- or polyunsaturated fats (MUFA or PUFA), where two or more double bonds indicate the latter. The double bonds in UFAs are in cis-configuration, causing a bend in the chain preventing as tight packing as in SFAs. As a result, UFAs are liquid at room temperature. These are considered healthier fats and are found in foods such as avocado, peanuts and rapeseed oil. PUFAs have been shown to act as biological mediators, helping in reducing the risk of some cardiovascular

conditions [18].

TFAs contain at least one double bond, like UFAs, but differ in the configuration of the bond as it is in trans-configuration [19]. This results in a straighter chain, allowing for tight packing similar to SFAs, making them solid at room temperature. This property, as well as often being cheaper than the healthier fats, has made TFAs attractive in recent years in a variety of processed foods. While TFAs are found naturally in dairy or red meat, they are most commonly industrially produced through hydrogenation of UFAs, resulting in for instance margarine [1].

However, due to the health risks associated with TFAs, their use in food products is being restricted, creating a need for alternative fat structuring methods. As previously mentioned, gelled systems offer a promising approach to solidify healthier unsaturated fats without altering their chemical composition [20].

2.4 Protein

Proteins are long-chain polymers composed of amino acids that are linked through peptide bonds [21]. While most amino acids can be synthesized by the human body, essential amino acids cannot and must be supplied from food. Meat is a rich source of protein, with content varying depending on source and cut, typically containing 25-30 g per 100 g [22]. In plant-based meat analogues, common protein sources are pea, soy, and wheat gluten [2].

Green pea, *Pisum sativum*, is a legume containing protein, dietary fiber, starch, carbohydrates, minerals and vitamins [23]. Its protein content ranges from 21-25% per dry weight, while the primary component is starch, accounting for 55-68% per dry weight. Pea protein mostly consists of globulins (65-80%) and albumins (10-20%) and possess various favorable functional properties, such as good water solubility and effective emulsion and gelation abilities [24].

2.5 Emulsions

An emulsion consists of two immiscible phases with different polarities, typically an oil phase and a water phase, where one is dispersed within the other [25]. They are classified based on the phase distribution, either O/W or W/O. Due to the large

interfacial area between the phases, emulsions are thermodynamically unstable [26]. The stability can be improved by addition of emulsifiers, typically hydrocolloids or proteins, which are surface active agents (surfactants) that prevent phase separation by hindering the dispersed droplets from merging together, avoiding droplet coalescence [27]. Additionally, the droplet size could be mechanically adjusted, through mixing with high shear forces.

Emulsions are widely used in the food industry as delivery systems as they possess the ability to effectively encapsulate functional food ingredients such as bioactive lipids, antioxidants and flavors, of both hydrophilic and hydrophobic nature [28]. However, they lack the necessary structuring and mechanical properties to effectively mimic animal fat.

2.6 Gels

Gels are three-dimensional network materials primarily consisting of two components, a liquid medium and a dispersed solid network [3]. They simultaneously exhibit both viscous (fluid-like) and elastic (solid-like) properties, resulting in its viscoelastic nature [29]. The network consists of molecules commonly referred to as gelling agents or gelators, which are typically proteins, polysaccharides, or polymers. To form a gel, these compounds are dispersed in a medium such as water (hydrogel), oil (oleogel) or air (aerogel). The networks are bound through different interaction types, including hydrogen, ionic and covalent bonds as well as hydrophobic interactions, with gel strength dependent on the interaction. In soft gels, the crosslinks are able to break and reform, whereas those in hard gels are permanent and unable to recover once disrupted.

In contrast to emulsions, gels are often used in the food industry due to their structuring and mechanical properties. However, single phase gels lack the combined properties of both water and oil phases, limiting their functionality in applications where both hydrophilic and lipophilic properties are required.

To overcome the limitations of emulsions and gels respectively, various formulations have been developed, gaining increased attention in food applications in recent years. Among these, emulsion gels and bigels have emerged as promising systems. These allow for the structuring of liquid oils into a more solid form, thereby improving

stability, texture and functionality.

2.6.1 Emulsion gels

In emulsion gels, also termed emulgel, the emulsion is embedded in a gel network [4]. The preparation typically involves two steps: first, the emulsion is formed, and then the gelling occurs by either aggregating the dispersed phase or gelling the continuous phase through various mechanisms.

By incorporating gels into emulsions, emulsion gels offer advantages over their individual components [30]. The result is improved stability against physical processes, such as phase inversion and separation as well as environmental changes like pH and temperature. Additionally, the oil phase in emulsion gels allows for the delivery of hydrophobic compounds, addressing a major limitation of hydrogels [25]. When distributed in gels, functional ingredients are better protected, enhancing the efficiency of food additives, bioactive compounds, and lipophilic nutrients compared to when distributed in traditional emulsions [26][30]. These molecules often exhibit low stability and water solubility, which complicates their incorporation into food products. Because of the compact gel structure in the hydrogel phase, emulsion gels are also able to deliver hydrophilic functional ingredients [26]. Emulsion gels can also be tailored to behave differently in response to environmental conditions, enabling control over when incorporated functional ingredients are released and increasing their bioavailability.

However, while emulsion gels overcome some limitations of both emulsions and gels, they still face challenges. Their mechanical properties and oil structuring ability may not always be suitable to fully mimic the behaviour of animal fats, and they could exhibit some phase separation over time. Thus, to further improve the functionality of structured fat systems, bigels have been developed.

2.6.2 Bigels

Bigels, a relatively new technique for structuring oils in the food industry, are a mixed system of two gel phases of different natures, typically a hydrogel and an oleogel, which combine properties of each phase [4][3]. Similar to emulsions, bigels can be classified as O/W, where the oleogel is dispersed within the hydrogel phase,

or vice versa, as W/O [31].

According to a review by Shakeel et. al., the most critical factors for bigel preparation include mixing temperature and speed, storage conditions, constituents of the hydrogel and oleogel and their ratio [3]. An increasing oleogel content affects multiple parameters, such as viscosity and firmness, whereas the effect of higher hydrogel ratios on bigel hardness depends on the specific gel systems and their interactions.

Key characteristics of bigels include enhanced stability at room temperature compared to the two phases separately, as well as the ability to easily manipulate the desired properties by adjusting their ratio. Bigels possess multiple favorable and unique characteristics, for instance the possibility to deliver both hydrophobic and hydrophilic agents owing to the polarity of the two phases, good spreadability, and easy preparation [32]. Since both phases are gelled, they possess higher stability compared to emulsion gels, single-phase gels and emulsions, thereby enhancing texture and structural integrity in food products.

2.7 Texturizers

Polysaccharides, a group of hydrocolloids, are long-chained carbohydrate macromolecules composed of monosaccharides monomers [33]. The monosaccharide units are linked through α- or β-glycosidic bonds, enabling the formation of various polysaccharides with different properties and functions, either branched or linear in structure.

Only some polysaccharides are capable of gel formation, which occurs once their concentration reaches a specific level termed the critical concentration [29]. The polysaccharide is then referred to as a gelling agent. Polysaccharides that lack gelling ability are used for other purposes, mainly as thickeners or stabilizers. The polysaccharide can be classified as either coldsetting or heatsetting, depending on their gelling mechanism [34].

2.7.1 Agar

Agar is a linear polysaccharide found in the cell wall of red algae and is widely used in food applications as gelling agent [35]. It consists of agarose and agaropectin,

where the first being the primary gelling component [36]. Agar exhibits excellent gelling properties and high water solubility [29][33], and is considered a coldsetting polysaccharide, as the gel sets upon cooling [36]. In 3DP applications, agar mainly contributes through its shear-thinning abilities and capacity to enhance viscoelasticity [2].

2.7.2 κ-carrageenan

Just like agar, κ-carrageenan is a linear polysaccharide derived from red algae, but with repeating units of D-galactose and 3,6-anhydro-galactose [33]. Beyond kappa, there are several other types of carrageenan, for instance iota and lambda, which differs in unit numbers and the positioning of sulfate side groups. Among these three types, only kappa and iota form gels, whereas lambda is used as a thickener [29]. κ-carrageenan forms strong and brittle gels in the presence of cations [37]. It also possesses shear-thinning properties, making it beneficial for 3DP [2].

2.7.3 Xanthan gum

Unlike agar and κ-carrageenan, xanthan gum is a branched polysaccharide derived from bacteria, composed of D-mannose, D-glucose and D-glucuronic acid [33]. Xanthan gum is not by itself considered a gelling agent, but can together with other polysaccharides form high-quality gels [29]. It is also one of the most widely used thickeners in the food industry [33]. In 3DP, xanthan gum has proven to improve printability through its shear-thinning properties [2].

2.7.4 Beeswax

Beeswax, also known as Cera alba, is a natural wax produced by bees [38]. The primary component is esters of higher fatty acids and alcohols, and it is stable and insoluble in water. At room temperature, beeswax is solid, but becomes brittle below 18 °C and soft over 35 °C. Its melting point varies depending on composition, but generally ranges between $60 - 70$ °C. Due to its versatile properties, beeswax is widely used in food, cosmetics and pharmaceuticals industries.

2.8 3D printing

Food 3DP is an emerging technology offering new opportunities in the production of novel sustainable plant-based meat analogues due to its precision and ability to replicate complex structures and textures [2]. Various printing techniques are available, including inkjet and binder jetting, but the most widely used in food 3DP is extrusion based [39].

In extrusion based 3DP, the material is deposited layer by layer to create the desired object. The first step in the process involves the construction of a 3D model, typically done in a computer-aided design (CAD) software [2]. The object is then exported in STL format, a standard file type in 3DP, and converted into G-code using a 3D slicer software, which slices the object in horizontal layers. The G-code controls all aspects of printing, for instance the extrusion of material and movement of the printheads and bed. The food ink is loaded into a cartridge, and a plunger then applies force pushing the material through the attached nozzle, resulting in material deposition layer by layer to produce the desired shape of the food item.

In the printing process, there are multiple parameters influencing the outcome [40]. The factors with the greatest impact on the result include extrusion width, layer height, nozzle diameter, extrusion multiplier, printing speed and printing temperature, all of which will be of importance in this study. These are adjusted in the slicer program and expressed in the G-code. The extrusion multiplier determines the volume of material that is pushed through the nozzle during printing. Another important concept is defined extrusion, which ensures smooth material deposition. This is achieved by adjusting the extrusion width to 1.5 times the nozzle diameter. An extrusion width smaller than this results in under extrusion, causing adhesion issues since there is not enough material to deposit.

The printability of a material can be described by combining the two key terms extrudability and buildability [41]. Extrudability is related to its ability to flow, correlated to the extrusion out of the nozzle, whereas buildability is related to the rheological properties after deposition. Good extrudability allows the material to flow easily under applied pressure, but stops once the force is removed. Likewise, with good buildability, a material is able to support additional layers deposited on top without collapsing, exhibiting resistance to deformation.

Advantages of using 3DP in food applications involve the precision and ability of quickly implementing new designs and optimizing the printing parameters [2]. A single printer offers several possibilities, since it is not restricted to a single shape or material. The process can easily apply a trial-and-error approach. Compared to traditional methods in meat analog production, the number of unit operations can be reduced, saving energy and time. 3DP also enables developed mouthfeel sensations and complex structures, having the potential to overcome the difficulties in mimicking the marbling of meat.

2.8.1 Dual and coaxial extrusion

MM3DP provides a method for replicating the marbling of meat by enabling deposition of multiple materials simultaneously [6]. There are multiple techniques available, including dual and coaxial extrusion. This facilitates the incorporation of the structured fat systems with protein-rich inks.

In dual extrusion, two materials are extruded together through a single nozzle or two separate on the same printer [6]. When two nozzles are used, the materials are extruded independently, allowing for layered structures or side by side printing. A single shared nozzle enables the materials to be extruded simultaneously, resulting in a distinct interface between them in the extruded strand, see Figure 2.1a [42]. The ratio between the materials can be adjusted during the process and different printing parameters can be set based on the materials' properties.

Coaxial extrusion, on the other hand, involves the simultaneous extrusion of two materials through a single shared nozzle only [6]. The difference compared to dual extrusion lies in the distribution of the materials in the extruded strand, which in coaxial extrusion are arranged in a core-shell structure. The cross-section of the strand reveals two distinct layers, with one forming the core layer and the other a surrounding shell, see Figure 2.1b [42].

(a) Dual extrusion (b) Coaxial extrusion

Figure 2.1: Cross-sectional area of extruded strands using different extrusion methods. The illustrations show material distribution within the strand, where the beige area represents the gel system and the pink the protein-rich ink.

2.8.2 Custom extrusion module

For this study, a custom mixing module prototype was used, developed in collaboration between FELIXprinters and Chalmers University of Technology, see Figure 2.2.

Figure 2.2: A prototype of the custom-made mixing module, constructed in plastic with interchangeable components. The left configuration illustrates the dual extrusion mode, where two materials are deposited side by side. The right configuration shows the coaxial extrusion mode, in which one material is extruded through a core surrounded by the second material.

The prototype was made of plastic, but the final version will be constructed in stainless steel and therefore enhance the thermal stability of the module, ensuring a more consistent material temperature during printing. The module is attached to the two cartridges in the 3DP, allowing the different materials to be directed through separate pathways within the module. Through interchangeable inner components, the module is designed to enable switching between the two modes. Figure 2.2 displays the mixing module with the two different configurations, dual (left) and

coaxial (right) extrusion.

2.8.3 Food inks in literature

Several food ink formulations have been explored in the literature to advance the development of plant-based meat analogues.

In a study by Badager, two different forms of pea protein, isolate (PPI) and concentrate (PPC), were investigated at varying concentrations to evaluate their suitability for 3DP [43]. The rheological properties and printability were examined, concluding that PPI at 30 wt% was printable with decent resolution. In contrast, PPC was not printable by itself, however, the addition of pectin enabled successful printing at 40 wt%.

A study by Qiu *et al.* investigated bigel inks for food 3DP with different ratios of hydrogel and oleogel, through the e valuation of printability, rheological characteristics and microstructure [32]. The oleogel was composed of beeswax and corn oil, while the hydrogel contained κ-carrageenan, xanthan gum and distilled water. The results indicated that increased proportions of oleogel improved the mechanical strength and rheological properties, thereby enhancing the suitability for food 3DP. A key finding was that an 80% oleogel fraction provided optimal printability.

Zhu *et al.* studied the suitability of thermally reversible emulsion gels for food 3DP by evaluating different oil volume fractions [44]. Their research investigated the microstructure, rheological properties and printability of the gels. The emulsion gel was formulated using different concentrations of PPI, as well as different canola oil volume fractions. An oil volume fraction of 0.4 was found to result in optimal 3DP performance.

These studies highlight the effect of optimizing ingredients and tuning rheological properties to develop printable food inks with good performance. Based on these insights, the formulations in this study are designed by considering the identified key parameters.

2.9 Rheology

Rheology is the study of deformation and flow of materials, describing how their mechanical properties respond to applied stress or strain [45]. These properties are crucial in many areas, including food applications, cosmetic products and pharmaceuticals. In food 3DP, rheology is of great importance as it offers a pre-evaluation of a material's printability [46].

2.9.1 Rheological properties in relation to the 3D printing process

As earlier mentioned, the 3DP performance is directly influenced by the rheological properties of a material and the 3DP process can be divided into four stages: flow initiation, flow through the nozzle, deposition and layer support [47][2].

2.9.1.1 Flow initiation

The first stage of the 3DP process involves initiating a flow by applying force from a plunger, transitioning the material in the cartridge from resting to a flowing state [2]. Key parameters in this step involve yield stress, which is the amount of force or stress needed for a material to begin to flow, and low-to-medium viscosity [48][47]. Another important factor is the zero-shear viscosity, which is the viscosity of a material as the shear rate approaches zero [2].

2.9.1.2 Flow through the nozzle

In the second stage, the material must flow smoothly through the nozzle [2]. Low viscosity is of importance for the material to continuously flow. A key rheological property influencing this is shear-thinning behaviour, which is signified by decreasing viscosity with increasing shear rate, but once the applied force is removed the viscosity recovers [47]. In contrast, shear-thickening or Newtonian fluids, whose viscosity increases or remains unaffected by increasing shear rate, are not desirable as it prevents the material from flowing.

2.9.1.3 Deposition

During material deposition from the nozzle, quick recovery once the force is removed is crucial, restoring its viscosity and mechanical strength to maintain the desired shape and avoid spreading of the material [2]. This behaviour is related to

thixotropy, which, according to Mewis and Wagner, is defined as "the continuous decrease in viscosity with time when flow is applied to a sample that has previously been at rest and the subsequent recovery of viscosity in time when the flow is discontinued" [49]. Addition of thickeners can improve the recovery, through the formation of entangled polymer networks after deposition [50].

2.9.1.4 Layer support

Following deposition, the final stage of the 3DP process is layer support [2]. At this stage, the extruded ink should retain the desired shape, referring to the material's buildability. Recovery is also of importance in this stage, as well as yield stress, since the stress induced by the gravitational force from the layers above could potentially lead to deformation or collapse. Shorter recovery time indicates higher buildability, as it suggests that the material recovers faster after extrusion, providing support for subsequent layers [47].

2.9.2 Rheological tests

To evaluate the stages of the 3DP process, rheological analyses are conducted to gain insight into a material's behaviour under the different conditions. These tests are typically performed using a rheometer and are categorized as either rotational or oscillatory depending on the movement of the measuring probe [45].

The rheological analyses relevant for this study will be described in the following sections.

2.9.2.1 Amplitude sweep

Amplitude sweeps are commonly used to characterize the solid and liquid structural behaviour of food materials [48][45]. The test is conducted by varying the amplitude of either the oscillatory stress or oscillatory strain, while temperature and frequency are set to constant values. These are referred to as stress amplitude sweep and strain amplitude sweep respectively. The key outputs are storage modulus (G') and loss modulus (G") of the examined material.

The storage modulus, also referred to as the elastic modulus, describes a material's elastic (solid-like) behaviour and indicates the amount of energy stored during

deformation [48]. The loss modulus, or viscous modulus, on the other hand, characterizes the viscous (liquid-like) behaviour and represents the amount of energy dissipated as heat during deformation. Most materials exhibit both moduli, with the dominant modulus determining the overall behaviour. A high storage modulus indicates a stiffer gel structure and high stability after printing.

Another key objective of amplitude sweeps is to determine a material's linear viscoelastic region (LVE) [48]. The LVE is significant because the structure of the sample remains undamaged in this range. It is typically found at low amplitudes, where the storage and loss moduli exhibit plateau values. The upper limit of the LVE is defined at the point where either modulus noticeably deviates from their plateau, and can be determined either visually or with the help of software programs [45].

The critical strain (γ_L) is the limiting value that denotes the upper limit of the LVE in a strain amplitude sweep [45]. The yield point, or yield stress (τ_y), is the critical stress that marks the LVE end in a stress amplitude sweep. Although a stress amplitude sweep was not conducted in this study, the critical strain (γ_L) obtained from the strain amplitude sweep provides an indication of the material's yield stress. Additionally, the flow point, or flow stress (τ_f), occurs at the crossover point in a stress amplitude sweep, indicating the transition between solid-like and liquid-like behaviour.

2.9.2.2 Shear viscosity test

A shear viscosity curve measures the viscosity of a material against applied shear rate, providing information about the material's tendency to flow under different shear conditions [45]. Newtonian fluids are independent of applied shear rate, hence represented by a horizontal line, indicating constant viscosity. A gradual decrease in viscosity indicates a shear-thinning material, with increasing ability to flow with increased shear rates. A positive slope indicates a shear-thickening fluid. As previously mentioned, the shear-thinning behavior is crucial in 3DP, as it influences both extrusion and deposition stages.

2.9.2.3 Frequency sweep

Frequency sweeps measure storage and loss moduli by applying an oscillating frequency ramp, while keeping temperature and amplitude at constant values [45]. This method provides an understanding of a gel's strength and is performed within the LVE of the material. In soft gels, storage and loss moduli are highly dependent on frequency, often exhibiting a crossover point [48]. Semi-hard gels typically do not exhibit a crossover point but may still show some frequency dependence, with the storage modulus remaining dominant. The moduli in hard gels are independent of frequency, indicating a stable structure.

2.9.2.4 Three interval thixotropy test

The thixotropic behaviour of a material can be evaluated by performing a three interval thixotropy test (3ITT) [45]. The sample is subjected to three shear rate intervals, simulating different phases in 3DP [51].

In the first interval, a low shear rate is applied within the LVE, resembling the resting state in the cartridge. The goal is to obtain constant values for either storage and loss moduli or the complex viscosity (η^*), depending on which parameter is extracted from the test. The complex viscosity describes a material's viscoelastic behaviour [48]. For the second interval, a higher shear rate outside of the LVE is applied, simulating both flow initiation and extrusion through the nozzle. The third and final interval replicates material deposition and layer support, returning to the low shear rates applied in the first interval while remaining within the LVE.

2.9.2.5 Temperature sweep

In a temperature sweep, frequency and amplitude are kept at constant values, while varying temperature to gain insights into the thermal behaviour of a material through change in storage and loss moduli [45]. By performing the temperature sweep in heating and cooling cycles, an insight into a material's thermal stability and reversibility will be obtained.

A plateau in the storage modulus indicates structural stability with an intact gel network, while a descent or ascent demonstrates changes in structure [52]. A crossover point, where the moduli intersect, suggests a gel-to-sol or sol-to-gel transition. The temperature at which this occurs is referred to as the gelation temperature [53].

2.10 Confocal laser scanning microscopy

Confocal laser scanning microscopy (CLSM) is a widely used imaging technique in the food industry, allowing for visualization of microstructures, structural changes over time and the distribution of components [54]. Unlike traditional optical microscopy, CLSM utilizes a focused laser beam to scan the sample, without damaging the material.

To differentiate between components, the sample is stained with fluorescent dyes [54]. These bind to the proteins and fats respectively, allowing for a detailed image of microstructure and different phases. When subjected to the laser beam, the dyes absorb energy and transition to an excited state. As they return to the initial state, fluorescent light is emitted. These signals are then collected and filtered within a specific wavelength to produce the final image.

3 Methodology

The experiments were conducted in two phases. In the first, the suitability of the two gels as inks for food 3DP was evaluated and compared. The second part analyzed different MM3DP techniques, dual and coaxial extrusion, to assess the performance of the gels when printed together with a PPI-based ink.

3.1 Materials

A commercial PPI was used, NUTRALYS® F85M from Roquette, France. All polysaccharides, xanthan gum (CAS: 11188-66-2), κ-carrageenan (CAS: 11114-20-8) and agar (CAS: 9002-18-0) as well as beeswax (CAS: 8012-89-3) and citric acid (CAS: 5949-29-1) was purchased from Sigma-Aldrich. Rapeseed oil (EXTRA) was bought from Coop.

3.2 Study one: Evaluating emulsion gel and bigel in food 3D printing

3.2.1 Preparation of emulsion gel

The emulsion gel was prepared based on the method described by Zhu *et al.*, with modifications [44]. First, 15.7 wt% PPI and 2 wt% agar were thoroughly mixed before adding distilled water and then further mixed. Due to differences in protein purity between the PPI in the original study and this experiment, the PPI concentration was adjusted. The calculations are provided in the appendix, see Section A.1 in Appendix for details. Agar was added to further improve the viscoelastic properties of the emulsion gel. The pH was then adjusted to 3.4 using citric acid.

To create the emulsion, 40 ml rapeseed oil was homogenized with the protein solution using an Ultra-Turrax for 2 minutes at 20.000 rpm. The emulsion was then heated at 80 °C for 30 minutes in a shaking water bath (Julabo, SW22) to induce gelation.

After heating, the emulsion gel was transferred directly to the cartridge. A spoon was used to scoop out the emulsion gel due to its thicker consistency. The car-

tridge was then placed on ice for 30 minutes before being stored overnight in the refrigerator at 4 °C. All tests were performed the following day.

3.2.2 Preparation of bigel

The bigel was prepared following the method outlined by Qiu *et al.* [32], with some alterations presented in Section A.2 in Appendix. To form the hydrogel, a 1:1 ratio of κ-carrageenan and xanthan gum to total of 1.5 wt% was added to distilled water and heated at 99 °C in a shaking water bath (Julabo, SW22), for 40 minutes while stirred continuously at 200 rpm. The oleogel was formed by adding 15 wt% beeswax to rapeseed oil and heated at 80 °C, also stirred at 200 rpm for 40 minutes in a water bath on a heating plate.

After preparation of the two gels, both were put in the water bath (Julabo, SW22) and maintained at 99 °C to preserve their liquid state until mixing. The two phases were then homogenized, while placed in a water bath at 80 °C on a heating plate, using the Ultra-Turrax at 15.000 rpm for 2 minutes.

Following homogenization, the bigel was poured directly into the cartridge. The cartridges were then placed on ice for 30 minutes before being stored overnight at 4 °C in the refrigerator. All tests were conducted the following day.

3.2.3 Rheological analysis

The first step after preparation of the gels involved conducting the rheological tests in order to pre-evaluate their suitability for 3DP.

All rheological analyses were performed using the Paar Physica Rheometer MCR 300 (Anton Paar GmbH, Austria). Each test was conducted in duplicate for each sample. Parallel plate geometry PP25 with the TEK-150 plate and 1 mm gap was used. The data analysis software used was Rheoplus/32 V3.40.

After loading the sample, excess material extending beyond the edge of the measuring probe was trimmed. To prevent evaporation and ensure comparability between the tests, the edges were covered with a thin layer of mineral oil. Prior to each test, the samples were allowed to rest for a two-minute period.

3.2.3.1 Amplitude sweep

The strain was varied between 0.01% and 1000%, using an angular frequency of 10 rad/s at a constant temperature of 25 °C.

3.2.3.2 Shear-viscosity test

In the shear-viscosity test, the shear rate was varied logarithmically from 0.001 1/s to 100 1/s, while maintaining a constant temperature of 25 °C.

3.2.3.3 Frequency sweep

Based on the LVE results from the amplitude sweep, a strain of 0.01% was used. The frequency was varied between 200 rad/s to 0.1 rad/s and the temperature was set to 25 °C.

3.2.3.4 Three interval thixotropy test

In the first interval, a shear strain of 0.01% was applied during a period of 200 s, followed by an increase of the shear strain to 10% for 100 s in the second interval. For the last interval, the strain was once again decreased to 0.01% for 200 s. An angular frequency of 10 rad/s was used over all intervals and the temperature was maintained at 25 °C.

3.2.3.5 Temperature sweep

The temperature sweep was performed by subjecting the sample to a heating and cooling process. The heating ramp was conducted at a rate of 5 °C/min from 4 °C to 80 °C, followed by cooling from 80 °C to 4 °C at the same rate. A strain of 0.01% and frequency of 10 rad/s was applied.

3.2.3.6 Statistical analysis

The rheological data were plotted and statistically analyzed using MATLAB R2022b. For all replicates, the mean and standard deviation were calculated.

3.2.4 3D printing

3.2.4.1 3D printer and G-code creation

The 3D printer used in this study was custom-designed in collaboration between FELIXPrinters and Chalmers University of Technology. It was equipped with two cartridges, allowing for the simultaneous extrusion of two different materials. Both cartridges and bed were heatable. Additionally, a custom mixing module with interchangeable inner components was developed, designed to be mounted onto the cartridges, enabling switching between dual and coaxial extrusion modes.

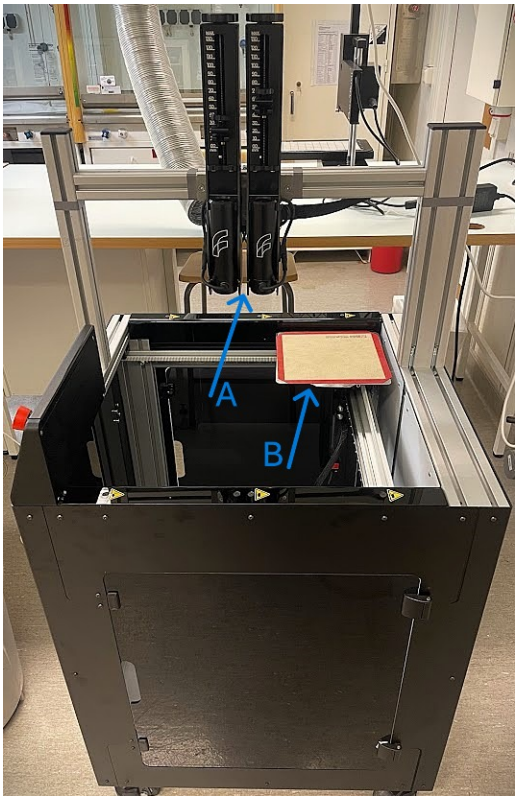

Figure 3.1: The 3D printer used in this study. A indicates the two cartridges, where the mixing module is attached. B marks the printing bed, moving in the x, y, and z directions during printing according to the G-code.

To construct the 3D models, AutoCAD was used for designing the shapes. Two models were created: a rectangular hollow tube and a solid rectangular cube, see Figure 3.2. The objects were saved in STL format and then imported to Simplify3D, a slicing software, where the two different objects' dimensions were adjusted to ensure they fit the desired printing pattern, before generating the G-code.

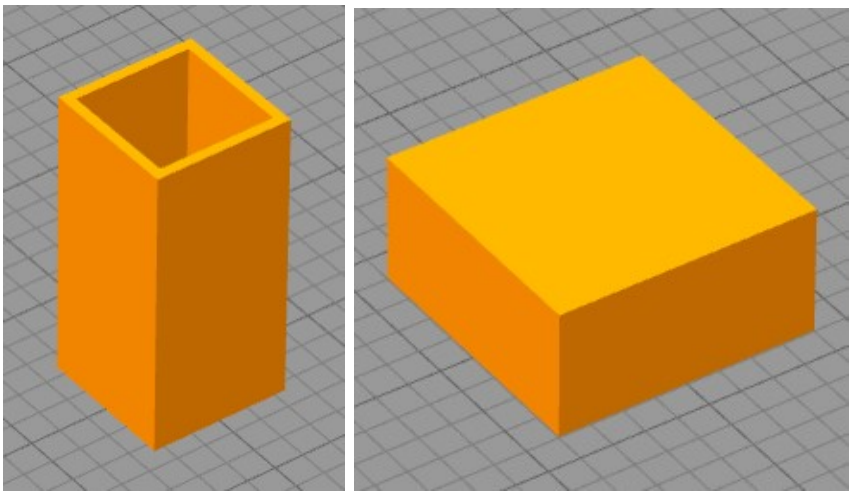

(a) rectangular hollow tube

(b) solid rectangular cube

Figure 3.2: The shapes constructed in AutoCAD used for the G-code.

3.2.4.2 Printing parameters

The printing parameters used for both gels in single printing are presented in Table 3.1. These values were selected based on prior experience with the material, on pre-studies where the parameters were optimized and on literature.

Table 3.1: 3D printing parameters used in study 1

Parameter	**Value**
Extrusion multiplier	1.25
Nozzle diameter	1.00 mm
Extrusion width	1.80 mm
Retract distance	1.00 mm
Extra restart distance	-0.05 mm
Retract speed	5.00 mm/s
Coasting distance	3.00 mm
Wiping distance	3.00 mm
Layer height	0.80 mm
First layer height	1.00 mm
First layer width	0.60 mm
First layer speed	15.0 mm/s
Default printing speed	25.0 mm/s

The printing temperature of emulsion gel was at room temperature whereas the bigel was set to 60 °C, which was found in a pre-study, see Appendix C.

3.2.5 Confocal laser scanning microscopy

CLSM was performed at RISE to analyze the phase distribution and microstructure of the gels.

Prior to conducting the CLSM, the samples were stained with FITC (Fluorescein isothiocyanate) for proteins and Nile red for lipids. No further preparation steps were required. The samples were then placed on a cover glass and placed in the inverted CLSM (Leica SP5), equipped with the objectives HC PL FLUOTAR 10.0x0.30 DRY and HCX PL APO lambda blue 20.0x0.70 IMM UV. Imaging was performed with a 488 nm laser, and emission signals were collected at 500-520 nm (green spectrum) for proteins and 570-610 nm (red spectrum) for lipids. Micrographs were captured at a resolution of 1024x1024 pixels.

3.3 Study two: Evaluating multi-material 3D printing

3.3.1 Preparation of PPI30

The PPI based ink (PPI30) was prepared according to Badager's method [43]. 30 wt% PPI and 5 wt% red food colouring, to resemble the colour of meat, was mixed with distilled water using a portable food chopper. However, when preparing samples for the CLSM analysis, no food coloring was used to prevent interference with the staining process. The food colouring and distilled water were mixed before adding to the PPI in the mixer. The samples were quickly blended to achieve optimal homogeneity, after which a spoon was used to manually mix the parts that the blades could not reach. The mixer was then sealed and left to rest for an hour to allow complete hydration.

After hydration, PPI30 was kneaded into cylindrical shapes and loaded into the cartridge. Plastic shock dampers were attached to the end of the cartridge, to facilitate the removal of air bubbles through tapping the cartridge. The ink was immediately available for printing.

3.3.2 3D printing

3.3.2.1 Printing process and parameters

To enable clearer visualization during MM3DP, some printing parameters were adjusted from study 1: the nozzle diameter, extrusion width, and layer height were increased from 1 mm to 4 mm. The G-code parameters presented in Table 3.2 were used for the dual extrusion investigation.

Table 3.2: 3D printing parameters used in study 2

Parameter	**Value**
Extrusion multiplier	1.25
Nozzle diameter	4.00 mm
Extrusion width	4.00 mm
Retract distance	1.00 mm
Extra restart distance	-0.05 mm
Retract speed	5.00 mm/s
Coasting distance	3.00 mm
Wiping distance	3.00 mm
Layer height	4.00 mm
First layer height	1.00 mm
First layer width	0.60 mm
First layer speed	15.0 mm/s
Default printing speed	25.0 mm/s

For the coaxial extrusion, however, the strands were extruded manually with the 4 mm nozzle and later cut to examine their cross-sectional structure, as this was proven to improve the evaluation process.
The printing temperature of emulsion gel as well as PPI30 was at room temperature whereas the bigel was set to 40 °C, which was found in a pre-study, see Appendix C.

3.3.3 Confocal laser scanning microscopy

The CLSM analysis in study 2 was conducted using the same methodology as described in Section 3.2.5. The only difference was that this analysis involved samples composed of two combined materials: PPI30 and either emulsion gel or bigel.

3.4 Photographic documentation

The objects were printed on the removable stainless steel plate on the printing bed and photographed in a portable mini studio (Foldio3, ORANGEMONKIE Inc) against a white background to ensure optimal contrast for documentation. The cut segments of the extruded strands in the coaxial extrusion analysis were photographed

against a blue background to enhance visibility. All images were captured using an iPhone 12 Pro.

4 Results and discussion

4.1 Study one: Evaluating emulsion gel and bigel in food 3D printing

The first study evaluated and compared the rheological and structural properties of the emulsion gel and bigel respectively. Rheological tests were performed to characterize their mechanical behaviour under different conditions. Performance in 3DP were evaluated, along with microstructure analysis using CLSM. The results are presented in the following sections.

4.1.1 Rheological properties

The rheological analysis included amplitude sweep, shear viscosity test, frequency sweep, three interval thixotropy test and temperature sweep. The results are presented in Figure 4.1.

4.1.1.1 Amplitude sweep

Figure 4.1a presents the amplitude sweep results for the bigel and emulsion gel, respectively. The LVE range for the bigel appeared to be much narrower in comparison to the emulsion gel, indicating that the bigel enters the non-LVE region at lower strains. This could suggest a less intact gel network, whereas the emulsion gel demonstrates a network that resists structural breakdown more effectively. Furthermore, a higher storage modulus was observed for the bigel, suggesting a stiffer structure and probably higher stability after printing. The yield stress is higher for the emulsion gel compared to the bigel, due to its wider LVE range, indicating that a greater applied force is necessary to initiate a flow.

4.1.1.2 Shear viscosity test

Both gels exhibit shear-thinning behaviour, see Figure 4.1b, characterized by the decrease in viscosity as the shear rate increases. However, the bigel has a steeper descent of the curve, indicating stronger shear-thinning properties. Additionally, the bigel exhibits a significantly higher initial viscosity. However, aligning with its previously observed lower yield stress, it begins flowing at lower shear rates.

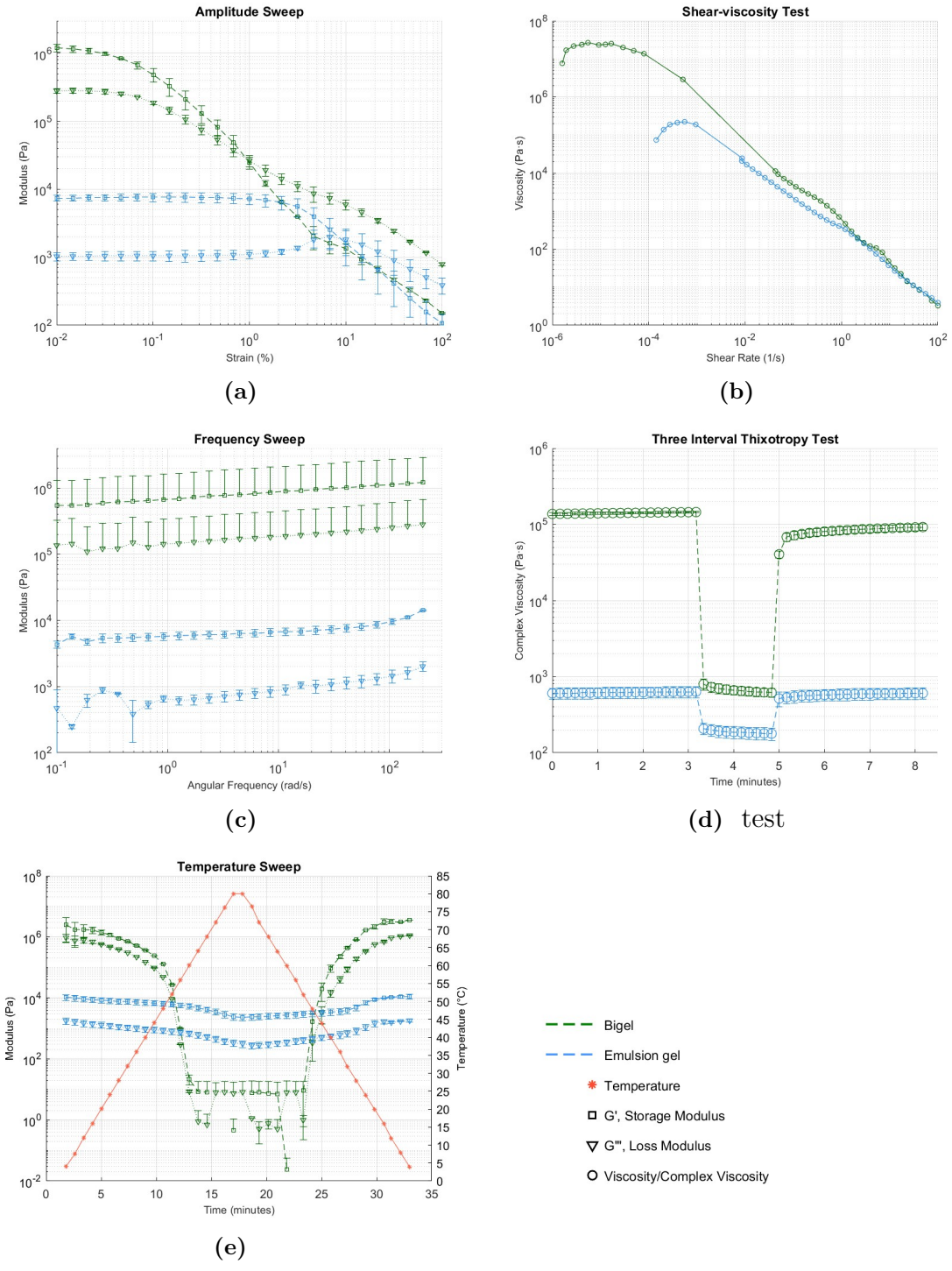

Figure 4.1: Results from rheological tests performed on the emulgel and bigel: (a) amplitude sweep, (b) shear viscosity test, (c) frequency sweep, (d) three interval thixotropy test, and (e) temperature sweep.

4.1.1.3 Frequency sweep

The storage modulus was constantly greater than the loss modulus for both samples and no crossover points were observed in either gel, indicating that neither gel is

considered (very) soft, see Figure 4.1c. However, the emulsion gel exhibited a small dependency of higher frequencies, which suggests it having a softer nature than the bigel. The deviations observed at low frequencies are most likely due to the rheometer's sensitivity.

4.1.1.4 Three interval thixotropy test

Both samples exhibited thixotropic behaviour, as shown in Figure 4.1d. The complex viscosity was consistently higher for the bigel across all intervals, indicating a stronger resistance to flow at rest. Entering the second interval, with applied strain in the non-linear region, both samples display a sharp decrease in complex viscosity, which is expected since they both showed shear-thinning behaviour in the shear viscosity test. However, the drop in complex viscosity of bigel was much greater. This aligns with its previously observed lower yield stress.

Both gels demonstrated quick recovery after decreasing the applied strain, with emulsion gel recovering slightly faster. Additionally, the emulsion gel nearly returned to its initial complex viscosity, in comparison to bigel which only partially recovered. This indicates a more irreversible change in the structure of bigel.

4.1.1.5 Temperature sweep

In Figure 4.1e, the emulsion gel showed consistently higher values of storage modulus compared to loss modulus, indicating a dominant elastic behaviour. The moduli remained relatively stable, only displaying minor decreases before returning to their original values at the end of the cycle. This suggests high thermal stability.

In comparison, the bigel demonstrated a higher sensitivity to increasing temperature. During the temperature ramp, both moduli instantly started to decrease, with a sharp drop at approximately 50 °C, likely associated with a disruption of the gel network. A plateau in the storage modulus was observed between 60-80 °C, suggesting a temporary stabilization of the remaining network. After the cycle, both moduli recovered closely to their initial values, indicating significant recovery of the bigel, thereby showing its thermal reversibility.

These findings highlight the differences in thermal stability between the gels. The emulsion gel appears more thermally stable, whereas the bigel, on the other hand, is

more responsive to temperature changes, which might facilitate smoother extrusion at elevated temperatures.

4.1.2 3D printing

The gels were successfully printed using the same G-code, as shown in Figure 4.2. The optimal printing temperature for bigel was found to be 60°C in a preliminary study (see Figure C.3 in Appendix), while the emulsion gel remained unaffected by temperature changes (see Figure C.2), supporting the results from the temperature sweep in Section 4.1.1.5.

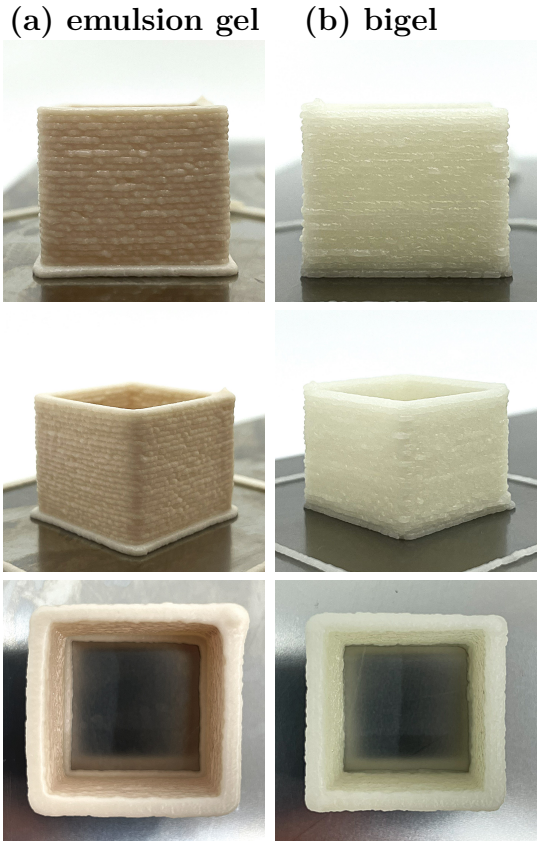

Figure 4.2: Printed objects of emulsion gel and bigel, displayed from the front, side, and top view. The same G-code and printing parameters were used for both gels.

As expected from the rheological analysis, both gels exhibited shear-thinning behaviour, which earlier mentioned is a critical property in 3DP. The printed objects of both gels showed good resolution, extrudability and buildability, as well as successfully retaining the shape after deposition. However, some structural differences between the two were observed. Bigel appeared to be more even in structure, with

smoother and more defined layers, in comparison to emulsion gel which exhibited a rougher texture. The softer nature of emulsion gel was evident during printing, as it appeared to be wobbling and instable, whereas bigel did not exhibit this behaviour.

To further evaluate the structural integrity, taller objects were printed in an initital pre-study, see Appendix D.1. While the bigel was capable of being printed at increased layer heights, it still exhibited poor resolution at higher layers. However, despite these irregularities in structure, the bigel successfully supported the additional layers without collapsing, unlike the emulsion gel which failed to withstand the same conditions. This demonstrates the superior self-supporting properties of bigel, but also highlights a need for optimization to improve resolution throughout the entire printed object.

The self-supporting properties of bigel are further confirmed in Figure D.2 in Appendix D.2. The printed object was placed on its side without deforming, still maintaining its shape despite lacking support from underlying layers. The structure can even withstand additional weight without deforming.

An important factor influencing the optimal printing temperature is the material of the mixing module prototype. Since it is constructed in plastic, the temperature of the material decreases as it travels through the module. This effect was particularly noticeable when extruding bigel too quickly, as it was extruded in a liquid state that rapidly solidified after deposition, see Figure C.1 in Appendix C. This further confirms the thermal reversibility of bigel, and suggests that the actual extrusion temperature at the nozzle during printing is lower than 60°C. When the final version of the mixing module in stainless steel is used, heat conservation is expected to improve, potentially shifting the optimal printing temperature.

Lastly, a significant difference in storage stability was observed between the gels. Since this was not a focus of the study, no precise time frame was recorded for the storage investigation. However, based on visual observations, the emulsion gel exhibited phase separation when left at room temperature over 1-2 days. After this time, visible oil leakage and water evaporation had occurred, leaving only a dry protein structure, see Figure D.3. In contrast, the bigel remained stable for at least a month, showing no apparent structural changes, see Figure D.2, which was captured approximately one month after printing. This highlights a superior storage stability

of bigel.

4.1.3 Confocal laser scanning microscopy

The CLSM results provide insights into the microstructure of both gels, as well as the effect of extrusion in 3DP, as displayed in Figure 4.3 and Figure 4.4.

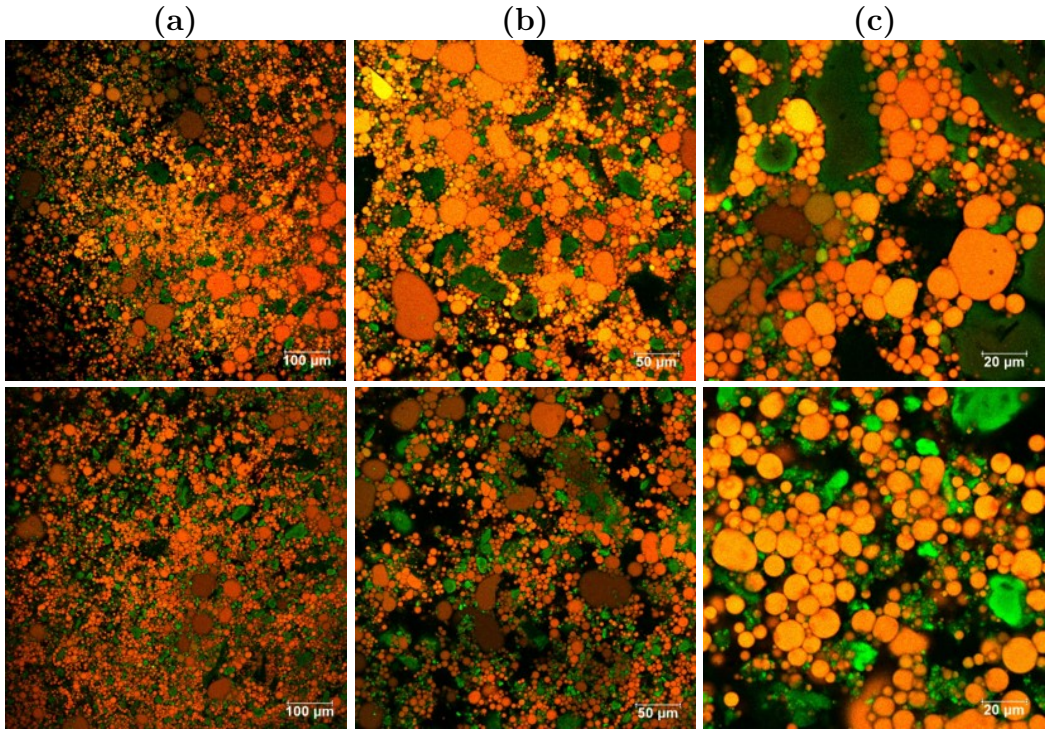

Figure 4.3: Confocal laser scanning microscopy images of emulsion gel, captured before (a–c) and after (d–f) 3D printing. The scale bars represent (a, d) 100 µm, (b, e) 50 µm, and (c, f) 20 µm.

Figure 4.3 presents the CLSM imaging of the emulsion gel before (upper row) and after (lower row) 3DP. The images display a typical emulsion distribution, with dispersed red lipid-rich oil droplets of varying sizes within the continuous green protein-rich hydrogel phase. This indicates an O/W distribution, which was expected due to the ratio of the two phases.

However, the presence of larger, irregularly shaped droplet clusters suggests partial phase separation, potentially due to insufficient protein network stabilization, resulting in poor emulsification. Compared to the findings in the study of Zhu *et al.* [44], the emulsion gel in this study appears less stable, which may be due to variations in PPI composition between the studies. Despite adjustments in concentration

to match the protein content, additional agar was still needed to improve emulsion stability. The bright green areas visible in the CLSM images likely represent aggregated protein clusters that were not uniformly dispersed in the hydrogel, failing to stabilize the interface between phases. Moreover, insufficient homogenization during sample preparation may have further contributed to the observed instability.

This structural weakness is consistent with the rheological measurements, where the emulsion gel exhibited a softer nature and weaker network compared to the bigel. This was also aligned with the 3DP performance, as the emulsion gel collapsed under increased layer height. Furthermore, the CLSM results also correspond to the observed storage instability of emulsion gel, as phase separation occurred rapidly.

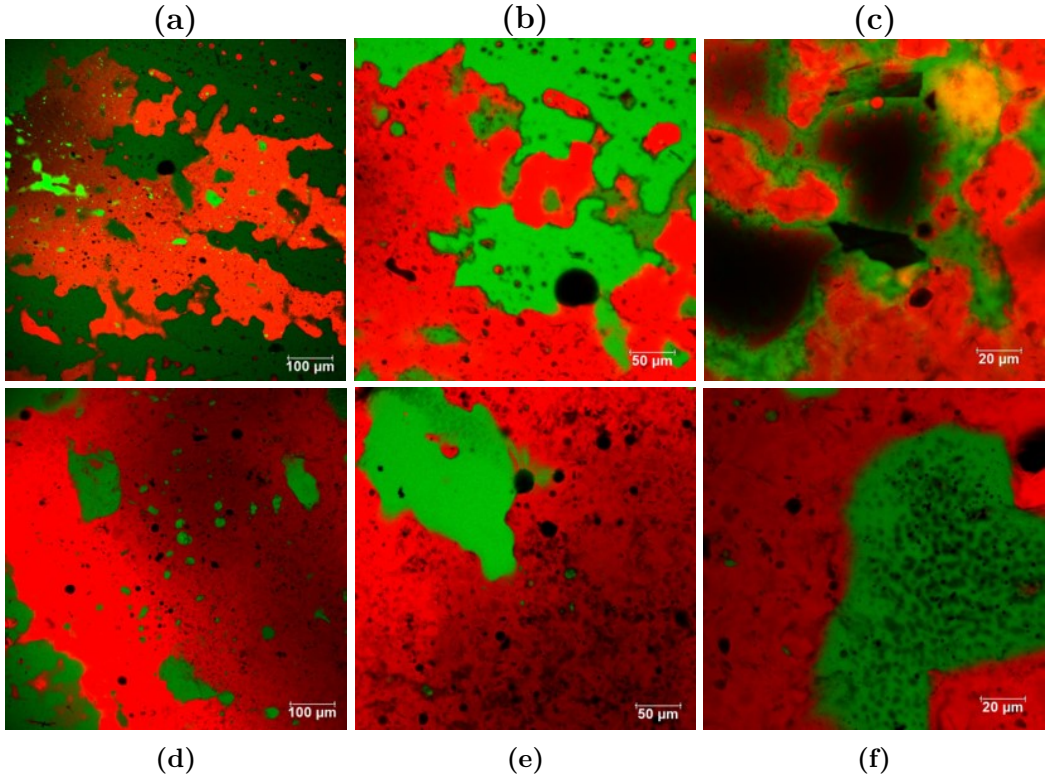

Figure 4.4: Confocal laser scanning microscopy images of bigel, captured before (a–c) and after (d–f) 3D printing. The scale bars represent (a, d) 100 µm, (b, e) 50 µm, and (c, f) 20 µm.

The CLSM results of the bigel shown in Figure 4.4 reveal a heterogeneous microstructure, exhibiting dominant lipid clusters forming the oleogel phase. The hydrogel phase is dispersed as clusters of smaller regions in the continuous oleogel phase. This confirms a W/O distribution, or hydrogel in oleogel structure. This was expected, due to the high ratio of oleogel compared to hydrogel, aligning with the

results from the study of Qui *et al.* [32]. These findings are also consistent with the rheological results, where the bigel exhibited a higher storage modulus and stronger gel network, contributing to its superior mechanical stability.

After printing, no visible changes in microstructure were observed for either of the gels, indicating that 3DP did not affect the phase distribution or disrupt the network. A similar observation was reported by Qui *et al.* [32], who connected this to the quick recovery characteristics and the highly ordered structure of bigel.

4.2 Study two: Evaluating multi-material 3D printing

The second study aimed to explore MM3DP using emulsion gel and bigel in combination with PPI30. The objective was to assess material compatibility and structural performance when printed in dual and coaxial configurations.

4.2.1 3D printing

In study two, a 4 mm nozzle was selected to improve the evaluation of material compatibility, owing to the larger cross-section area of the extruded strand. The increased diameter allowed for a clearer observation of how the gels behaved in combination with PPI30 in MM3DP.

4.2.1.1 Dual extrusion

The differences in MM3DP behaviour between the two gels were significant. In Figure 4.5a, the emulsion gel demonstrated poor printing performance, unable to maintain the desired 50:50 distribution along the printed lines. This suggests poor material compatibility with PPI30, likely due to differences in rheological properties. The weak gel network of the emulsion gel, revealed in study 1, is further confirmed by its visible smearing across the printing bed. A noticeable blending between the materials was also observed, suggesting that they have partially mixed, which is undesired and not intended.

Another critical issue was the irregular ejection of emulsion gel during extrusion. The emulsion gel was sporadically extruded in an uncontrolled manner during printing instead of smoothly alongside PPI30, as seen in Figure 4.5. This behaviour further confirms that the materials were not compatible, as they appeared to compete for

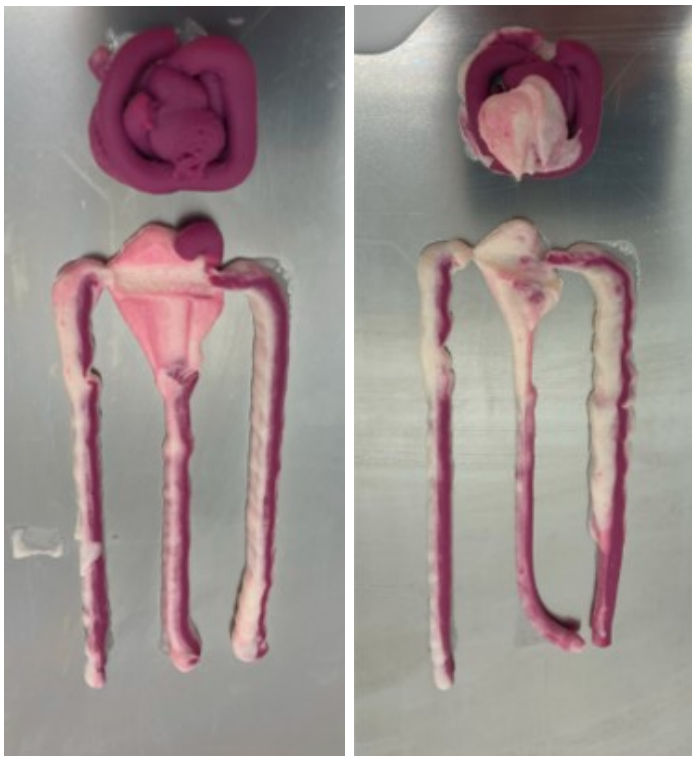

(a) 50% speed **(b)** 25% speed

Figure 4.5: Emulsion gel and PPI30 printed using a 4 mm nozzle at two different printing speeds in dual extrusion mode, (a) at 50% speed and (b) at 25% speed.

space in the extrusion pathway rather than forming a uniform strand. The purge cubes also confirm this incompatibility, as one is almost entirely composed of PPI30 instead of the expected 50:50 ratio before the line test.

On the other hand, the bigel exhibited a more stable dual extrusion process in combination with PPI30. However, when printed at 60°C, the optimal printing temperature for bigel in study 1, the results in Figure 4.6a revealed that the 4 mm nozzle caused the material to be extruded too quickly in comparison with the 1 mm nozzle, causing the material to be extruded at a too liquid state. This aligns with the observations in Figure C.1 in Appendix C, where the impact of the printing temperature on printability was evident. This was addressed by decreasing the temperature to 40°C, with two different extrusion speed settings. At 100% speed, displayed in figure Figure 4.6b, material compatibility was improved, while still exhibiting certain irregularities in material distribution across the lines. Furthermore, 50% speed resulted in a much smoother distribution, exhibiting close to 50:50 ratio across the entire strands, see Figure 4.6c.

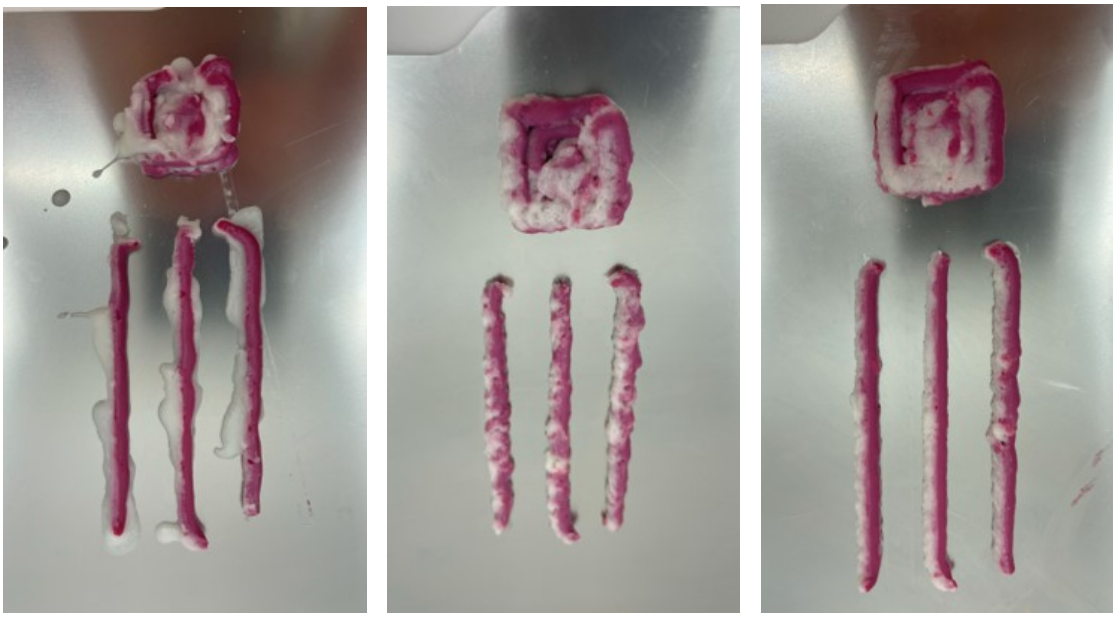

(a) 60°C at 100% speed **(b)** 40°C at 100% speed **(c)** 40°C at 50% speed.

Figure 4.6: Bigel and PPI30 printed in dual extrusion mode using a 4 mm nozzle under different printing conditions, (a) 60°C at 100% speed, (b) 40°C at 100% speed and 40°C at 50% speed.

Overall, the results from dual extrusion suggest that bigel performs better in terms of extrusion stability, material compatibility, and even distribution in combination with PPI30 compared to the emulsion gel. The emulsion gel demonstrated poor co-extrusion behaviour, with noticeable smearing and blending with PPI30, as well as unpredictable extrusion behavior, making it unsuitable for dual extrusion printing in its current formulation.

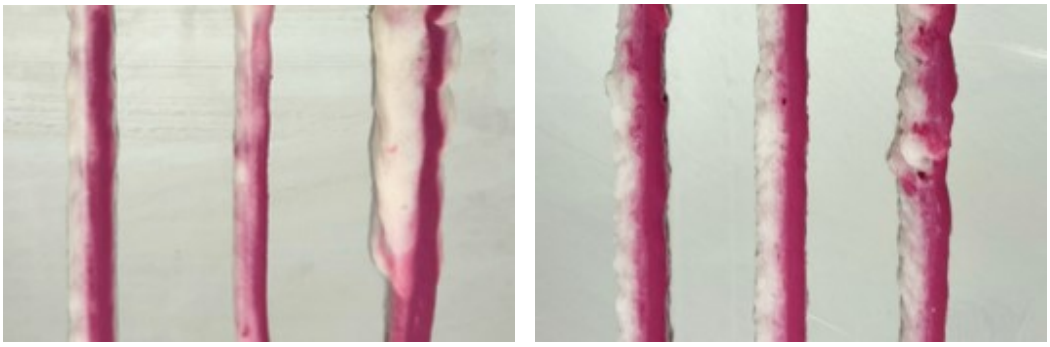

(a) Emulsion gel **(b)** Bigel

Figure 4.7: Zoomed-in images from the line test of dual extrusion multi-material 3D printing. The figure illustrates the differences in material distribution and the compatability between the gels and PPI30.

4.2.1.2 Coaxial extrusion

Figure 4.8 presents the results from MM3DP using the coaxial extrusion mode with PPI30 and either emulsion gel or bigel.

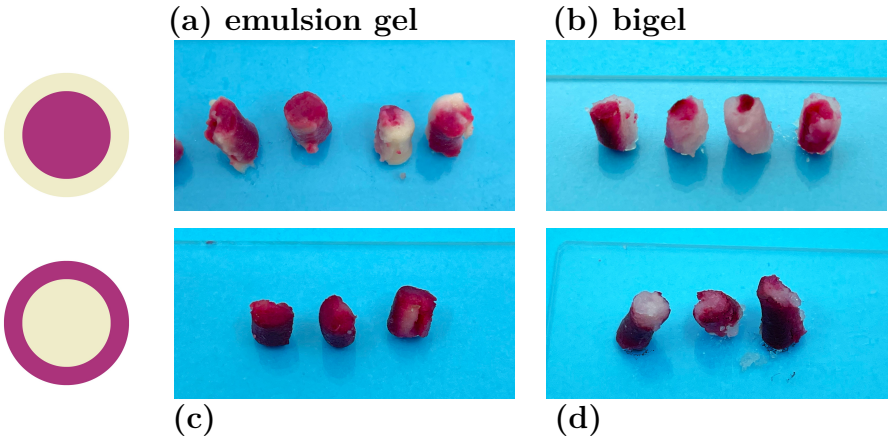

Figure 4.8: Results from multi-material 3D printing using the coaxial extrusion mode. The colored circles illustrate the configurations for each sample, where beige colour represents the gel and the pink is PPI30. The configurations is as follows: (a) emulsion gel outer, PPI30 inner, (b) bigel outer, PPI30 inner, (c) PPI30 outer, emulsion gel inner and (d) PPI30 outer, bigel inner.

Figure 4.8a displays the results of emulsion gel as the surrounding material and PPI30 as the inner core. The performance varied significantly among the cut segments of the extruded strands. While some segments appear to exhibit some surrounding behaviour, this is more likely to be random rather than controlled. Others display almost no emulsion gel, showing an uneven distribution along the extruded strand. The emulsion gel failed to form a continuous outer layer distributed over the strand. This inconsistency is likely due to differences in rheological properties between the emulsion gel and PPI30, as well as that the emulsion gel is significantly softer, and aligns with the results from dual extrusion. The emulsion gel did not provide a strong outer shell leading to an irregular pattern over the extruded strand.

The result from bigel as the surrounding material, as presented in Figure 4.8b, exhibited good integrity between the two materials with a clear distinction between the layers. The bigel effectively surrounded the core PPI30, while maintaining the round extruded shape and a consistent flow over the extruded strands.

With reversed material configuration, with PPI30 as the outer layer, the emulsion gel in Figure 4.8c is barely visible despite the set ratio being 50:50. This suggests that when PPI30 and emulsion gel were extruded coaxially, PPI30 dominated the process, much like what was observed in dual extrusion. Additionally, the emulsion gel also exhibited a tendency to leak through cracks in the mixing module instead of extruding smoothly through the nozzle, see Figure D.4. This observation suggests that the emulsion gel formula requires further optimization to improve its rheological properties. This issue could potentially also be improved by adjusting the printing parameters.

Figure 4.8d shows the results from bigel as the inner core material. Even in this configuration, bigel performed better, with clear boundaries between the layers further supporting its compatibility in MM3DP.

However, some limitations and sources of error must be taken into consideration. One challenge was the drying of PPI30 in some areas after 3DP, which may have influenced the visual evaluations. On the other hand, this should not have a huge impact on the results, since the drying primarily affected the color rather than the structural integrity between layers. Additionally, there were difficulties in cutting the samples, due to the soft nature of the gels. The emulsion gel samples were particularly hard to cut, as the softer texture made it more vulnerable to deformation, which probably impacted the cross-sectioning. Another factor was the variations in distribution along the extruded strand, making it challenging to obtain reliable results.

These findings further strengthen the suitability of bigel as a favourable animal fat substitute in MM3DP, while highlighting the need for further optimization of emulsion gel to improve its printability, stability and compatibility with PPI30.

4.2.2 Confocal laser scanning microscopy

To further investigate the differences between the gels in MM3DP with dual extrusion on a microstructural level, CLSM was conducted and presented in Figure 4.9.

Figure 4.9a-c displays the CLSM results of MM3DP of emulsion gel, where the interface appears not well defined, not a clear distinction between the two materials.

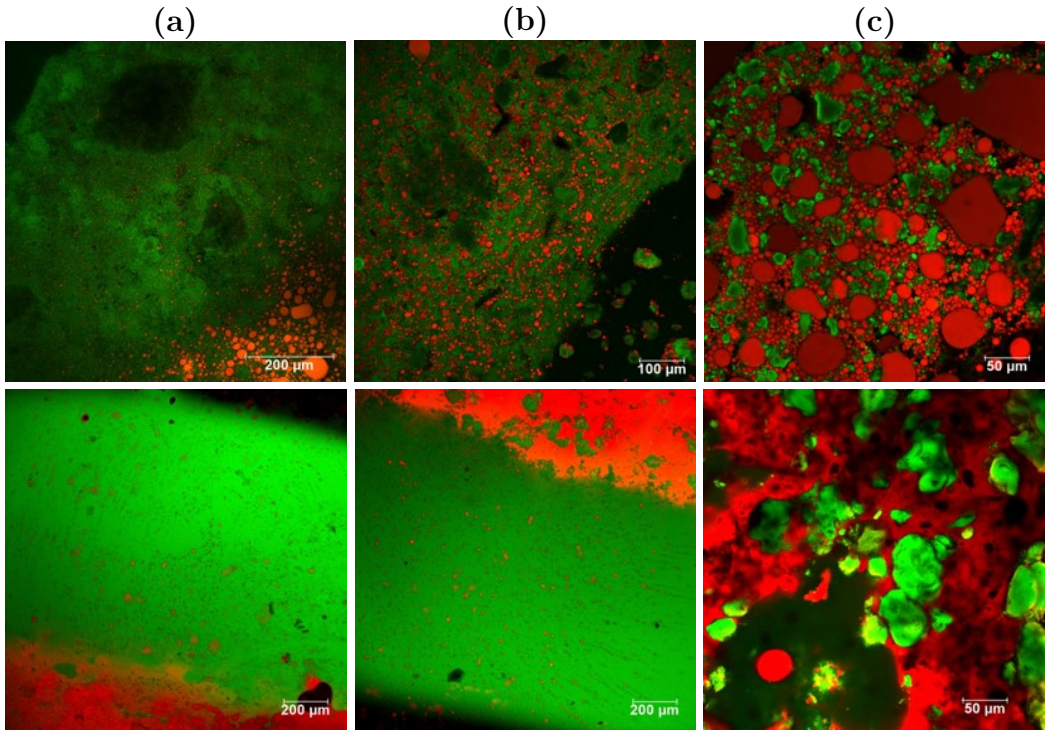

Figure 4.9: Confocal laser scanning microscopy images of multi-material 3D printing of PPI30 and emulsion gel (a-c) and bigel (d-f), respectively. The scale bars represent (a, d, e) 200 µm, (b) 100 µm, and (c, f) 50 µm.

A distribution of small oil droplets can be observed in the PPI30 phase, further proving the unstable structure of the emulsion gel. This was previously seen in the MM3DP results, see Figure 4.5a, where the two materials mixed during extrusion. This could potentially be due to smearing inside the nozzle, correlating with the unpredictable extrusion behaviour of emulsion gel observed during 3DP.

The challenges related to the weak structure of the emulsion gel were further evident during CLSM imaging. The sample was difficult to move, as adjusting its position on the cover glass risked smudging, limiting the ability to capture clear imaging. These findings confirm that the emulsion gel formulation used in this study is not suitable for MM3DP applications in its current state and that optimization is required to improve its rheological and structural properties.

The bigel, however, demonstrated a distinct interface where it remained confined to its intended region, see Figure 4.9d-f. This reinforces its superior integrity and compatibility with PPI30 in MM3DP compared to the emulsion gel, also corresponding

to the observed performance in previous tests. The CLSM results further validate that bigel is more suitable for MM3DP applications compared to emulsion gel.

5 Future outlook

First of all, one major challenge in this study was the instability of the emulsion gel, which exhibited phase separation and poor compatibility with PPI30 in printing. An optimization of the formulation would therefore be necessary in order to improve its structure and printability. When evaluating the two gels' suitability as animal fat substitutes in 3DP, the same printing parameters were used for both due to time constraints. Tailoring the parameters to each material's rheological properties would probably increase the printability and compatibility with PPI30 in MM3DP.

Further research should also improve the MM3DP extrusion methods and strategies of evaluation. In this study, the extrusion was assessed through visual evaluation of the cross-section of the strand, but the methods used were not optimal. By implementing advanced techniques, like cryosectioning, where the sample is frozen and sliced into thin sections without disrupting the structure, better insights on the materials' distribution would be available.

An interesting aspect found during the experiments, despite not originally being within the scope of the project, was the contrast in storage stability between the gels. Since this provides valuable insights in future product applications, it would be necessary to explore this further. Future research should evaluate the phase stability of the gels under room temperature, as well as under refrigeration and freezing conditions to gain deeper insights on performance during different situations the final product may encounter. Additionally, investigating post-processing techniques involving thermal treatments would be beneficial to evaluate how the gels interact with the food matrix in the final application.

Future research should also consider consumer acceptance, as it is one of the major challenges these products face. To address this, multiple parameters could be investigated. First, this study did not evaluate sensory properties such as taste, color, appearance and smell, all of which should be evaluated in order to enhance acceptability. The nutritional profile should also be assessed, since this plays a significant role in the customer acceptance.

Finally, comparisons with animal fat in all tested parameters; rheology, 3DP and

microstructure, would provide a more comprehensive understanding of how well the substitutes replicate animal fats.

6 Conclusion

This study explored the printability and structural performance of two fat structuring gel systems, emulsion gel and bigel, for potential application in food 3DP, with a focus on their suitability for food MM3DP.

The results demonstrated clear differences between the two gels. The emulsion gel showed a wider LVE range and higher yield stress, indicating good resistance to structural breakdown. However, it displayed poor structural stability under printing conditions, especially at increased layer heights, and was more prone to collapse and deformation. CLSM and storage tests revealed phase separation and instability, confirming that there are limitations of the emulsion gel in maintaining shape and structure over time.

In contrast, the bigel exhibited higher initial viscosity and stronger shear-thinning behaviour. While its LVE range was narrower, its printability was significantly better, producing more defined layers and could withstand increased layer heights. The bigel also demonstrated excellent self-supporting and storage properties, maintaining structural integrity under stress and over long storage periods. Its thermal reversibility further supports its suitability for 3DP processes involving elevated temperatures.

In MM3DP applications, the emulsion gel showed poor compatibility with pea protein, indicated by smearing, irregular extrusion and phase mixing. It failed to sustain a consistent 50:50 ratio during dual extrusion, as well as maintaining the desired core–shell structure during coaxial extrusion. In comparison, the bigel exhibited more distinct phase separation, more consistent dual extrusion and stronger core–shell formation, particularly under lower printing speeds and temperatures, highlighting their superior mechanical strength and structural integration with the pea protein isolate food ink.

Together, these findings highlight bigel's promising potential as a printable fat substitute in food 3DP. The emulsion gel requires further optimization to improve its stability and compatibility in printing applications.

References

[1] Bojana Bajželj, Federica Laguzzi, and Elin Röös. The role of fats in the transition to sustainable diets. *The Lancet Planetary Health*, 5(9):e644–e653, 2021.

[2] Elise Caron, Davy Van de Walle, Koen Dewettinck, and Flávio H Marchesini. State of the art, challenges, and future prospects for the multi-material 3d printing of plant-based meat. *Food Research International*, page 114712, 2024.

[3] Ahmad Shakeel, Ujala Farooq, Tanveer Iqbal, Saima Yasin, Francesca R Lupi, and Domenico Gabriele. Key characteristics and modelling of bigels systems: A review. *Materials Science and Engineering: C*, 97:932–953, 2019.

[4] Halil İbrahim KURT and Duygu KAVAK. Engineering sciences-2024.

[5] Weiwei Cheng, Jun-Hu Cheng, Da-Wen Sun, and Hongbin Pu. Marbling analysis for evaluating meat quality: Methods and techniques. *Comprehensive Reviews in Food Science and Food Safety*, 14(5):523–535, 2015.

[6] Yaxin Wen, Chhychhy Chao, Quang Tuan Che, Hyun Woo Kim, and Hyun Jin Park. Development of plant-based meat analogs using 3d printing: Status and opportunities. *Trends in Food Science & Technology*, 132:76–92, 2023.

[7] Hannah Ritchie, Pablo Rosado, and Max Roser. Environmental impacts of food production. *Our world in data*, 2022.

[8] PETA. Animals used for food, 2024.

[9] Rabia Shabir Ahmad, Ali Imran, and Muhammad Bilal Hussain. Nutritional composition of meat. *Meat science and nutrition*, 61(10.5772):61–75, 2018.

[10] Qiongling Chen, Zhenjia Chen, Jinchuang Zhang, Qiang Wang, and Yu Wang. Application of lipids and their potential replacers in plant-based meat analogs. *Trends in Food Science & Technology*, 138:645–654, 2023.

[11] Davide De Angelis, Atze Jan van der Goot, Antonella Pasqualone, and Carmine Summo. Advancements in texturization processes for the development of plant-based meat analogs: A review. *Current Opinion in Food Science*, 58:101192, 2024.

[12] Edirisingha Dewage Nalaka Sandun Abeyrathne, Kichang Nam, and Dong Uk Ahn. Analytical methods for lipid oxidation and antioxidant capacity in food systems. *Antioxidants*, 10(10):1587, 2021.

[13] Sayed Amir Hossein Goli, Mohammad Rezvani, and Maryam Abdollahi. Beeswax and monoglycerol-based oil foam: Effect of oil type and oleogelator concentration on physicochemical, rheological properties and storage stability. *Food Structure*, 37:100343, 2023.

[14] Alyssa Francavilla, Maria G Corradini, and Iris J Joye. Bigels as delivery systems: Potential uses and applicability in food. *Gels*, 9(8):648, 2023.

[15] Salvatore Coniglio, Maria Shumskaya, and Evros Vassiliou. Unsaturated fatty acids and their immunomodulatory properties. *Biology*, 12(2):279, 2023.

[16] Kevin C Maki, Mary R Dicklin, and Carol F Kirkpatrick. Saturated fats and cardiovascular health: Current evidence and controversies, 2021.

[17] Sujan Banik and M Hossain. A comparative overview on good fats and bad fats: Guide to control healthy body. *Int. J. Health Sci*, 2:41–44, 2014.

[18] Liana C Del Gobbo, Fumiaki Imamura, Stella Aslibekyan, Matti Marklund, Jyrki K Virtanen, Maria Wennberg, Mohammad Y Yakoob, Stephanie E Chiuve, Luicito Dela Cruz, Alexis C Frazier-Wood, et al. ω-3 polyunsaturated fatty acid biomarkers and coronary heart disease: pooling project of 19 cohort studies. *JAMA internal medicine*, 176(8):1155–1166, 2016.

[19] Vandana Dhaka, Neelam Gulia, Kulveer Singh Ahlawat, and Bhupender Singh Khatkar. Trans fats—sources, health risks and alternative approach-a review. *Journal of food science and technology*, 48:534–541, 2011.

[20] Ashok R Patel and Koen Dewettinck. Edible oil structuring: an overview and recent updates. *Food & function*, 7(1):20–29, 2016.

[21] Tom Coultate. *Food: the chemistry of its components*. Royal Society of Chemistry, 2023.

[22] Yuyan Yang, Yixin Zheng, Wenping Ma, Yin Zhang, Cuixia Sun, and Yapeng Fang. Meat and plant-based meat analogs: Nutritional profile and in vitro digestion comparison. *Food Hydrocolloids*, 143:108886, 2023.

[23] Edoardo Desiderio, Kavitha Shanmugam, and Karin Östergren. Plant based meat alternative, from cradle to company-gate: a case study uncovering the environmental impact of the swedish pea protein value chain. *Journal of Cleaner Production*, 418:138173, 2023.

[24] Parvathy Shanthakumar, Joanna Klepacka, Aarti Bains, Prince Chawla, Sanju Bala Dhull, and Agnieszka Najda. The current situation of pea protein and its application in the food industry. *Molecules*, 27(16):5354, 2022.

[25] Kelly Light and Salwa Karboune. Emulsion, hydrogel and emulgel systems and novel applications in cannabinoid delivery: A review. *Critical Reviews in Food Science and Nutrition*, 62(29):8199–8229, 2022.

[26] Yao Lu, Like Mao, Zhanqun Hou, Song Miao, and Yanxiang Gao. Development of emulsion gels for the delivery of functional food ingredients: From structure to functionality. *Food Engineering Reviews*, 11:245–258, 2019.

[27] Glyn O Phillips and Peter A Williams. *Handbook of hydrocolloids*. Elsevier, 2009.

[28] Like Mao, Yrjö H Roos, Costas G Biliaderis, and Song Miao. Food emulsions as delivery systems for flavor compounds: A review. *Critical Reviews in Food Science and Nutrition*, 57(15):3173–3187, 2017.

[29] A Nazir, A Asghar, and A Aslam Maan. Food gels: Gelling process and new applications. In *Advances in food rheology and its applications*, pages 335–353. Elsevier, 2017.

[30] Abdullah, Lang Liu, Hafiz Umer Javed, and Jie Xiao. Engineering emulsion gels as functional colloids emphasizing food applications: A review. *Frontiers in Nutrition*, 9:890188, 2022.

[31] Renata Miliani Martinez, Wagner Vidal Magalhaes, Bianca da Silva Sufi, Giovana Padovani, Lucas Idacir Sbrugnera Nazato, Maria Valéria Robles Velasco, Suzana Caetano da Silva Lannes, and Andre Rolim Baby. Vitamin e-loaded bigels and emulsions: Physicochemical characterization and potential biological application. *Colloids and Surfaces B: Biointerfaces*, 201:111651, 2021.

[32] Runkang Qiu, Kai Wang, Han Tian, Xuwei Liu, Guang Liu, Zhuoyan Hu, and Lei Zhao. Analysis on the printability and rheological characteristics of bigel inks: Potential in 3d food printing. *Food Hydrocolloids*, 129:107675, 2022.

[33] N Shafiei, M Nasrollahzadeh, and G Hegde. Biopolymer-based metal nanoparticle chemistry for sustainable applications. 2021.

[34] Jaekun Ryu and David Julian McClements. Impact of heat-set and cold-set gelling polysaccharides on potato protein gelation: Gellan gum, agar, and methylcellulose. *Food Hydrocolloids*, 149:109535, 2024.

[35] Xiaodan Chen, Xiaoting Fu, Luqiang Huang, Jiachao Xu, and Xin Gao. Agar oligosaccharides: A review of preparation, structures, bioactivities and application. *Carbohydrate Polymers*, 265:118076, 2021.

[36] Wei-Kang Lee, Yi-Yi Lim, Adam Thean-Chor Leow, Parameswari Namasivayam, Janna Ong Abdullah, and Chai-Ling Ho. Factors affecting yield and gelling properties of agar. *Journal of Applied Phycology*, 29:1527–1540, 2017.

[37] Ieva Bartkuvienė, Milda Keršienė, Vilma Petrikaitė, and Daiva Leskauskaitė. Modulation of pea protein isolate hydrogels by adding kappa-carrageenan: gelling properties and formation mechanism. *International Journal of Food Science and Technology*, 59(9):6598–6610, 2024.

[38] Yeshitila Eshete and Tekeba Eshetie. A review on crude beeswax mismanagement and lose: opportunities for collection, processing and marketing in ethiopia. *Journal of Nutritional Health & Food Engineering*, 8(6):384–389, 2018.

[39] Alain Le-Bail, Bianca Chieregato Maniglia, and Patricia Le-Bail. Recent advances and future perspective in additive manufacturing of foods based on 3d printing. *Current Opinion in Food Science*, 35:54–64, 2020.

[40] László Lendvai, Imre Fekete, Daniele Rigotti, and Alessandro Pegoretti. Experimental study on the effect of filament-extrusion rate on the structural, mechanical and thermal properties of material extrusion 3d-printed polylactic acid (pla) products. *Progress in Additive Manufacturing*, 10(1):619–629, 2025.

[41] P Wilms, K Daffner, C Kern, SL Gras, MAI Schutyser, and R Kohlus. Formulation engineering of food systems for 3d-printing applications–a review. *Food Research International*, 148:110585, 2021.

[42] Ivana M Cotabarren, M Itatí De Salvo, and Camila A Palla. Structuring food products using 3d printing: Strategies, applications, and potential. *Current Food Science and Technology Reports*, 1(2):109–121, 2023.

[43] Mikaela Isabel Badager. Evaluation of extrusion 3d printing of pea protein isolate and concentrate. Master's thesis, Chalmers University of Technology, Gothenburg, Sweden, 2024.

[44] Peineng Zhu, Yifu Chu, Jingqi Yang, and Lingyun Chen. Thermally reversible emulsion gels and high internal phase emulsions based solely on pea protein for 3d printing. *Food Hydrocolloids*, 157:110391, 2024.

[45] Thomas G Mezger et al. *The rheology handbook*, volume 10. Vincentz Network Hannover, Germany, 2012.

[46] PA Amorim, MA d'Ávila, R Anand, P Moldenaers, P Van Puyvelde, and V Bloemen. Insights on shear rheology of inks for extrusion-based 3d bioprinting. *Bioprinting*, 22:e00129, 2021.

[47] Zhenbin Liu, Bhesh Bhandari, Sangeeta Prakash, Sylvester Mantihal, and Min Zhang. Linking rheology and printability of a multicomponent gel system of carrageenan-xanthan-starch in extrusion based additive manufacturing. *Food Hydrocolloids*, 87:413–424, 2019.

[48] Helen S Joyner. *Rheology of semisolid foods*. Springer, 2019.

[49] Jan Mewis and Norman J Wagner. Thixotropy. *Advances in colloid and interface science*, 147:214–227, 2009.

[50] Arianna Dick, Xiuping Dong, Bhesh Bhandari, and Sangeeta Prakash. The role of hydrocolloids on the 3d printability of meat products. *Food Hydrocolloids*, 119:106879, 2021.

[51] Omer Said Toker, Salih Karasu, Mustafa Tahsin Yilmaz, and Safa Karaman. Three interval thixotropy test (3itt) in food applications: A novel technique to determine structural regeneration of mayonnaise under different shear conditions. *Food Research International*, 70:125–133, 2015.

[52] Gorjan Stojkov, Zafarjon Niyazov, Francesco Picchioni, and Ranjita K Bose. Relationship between structure and rheology of hydrogels for various applications. *Gels*, 7(4):255, 2021.

[53] JV Alemán, Alan V Chadwick, J He, M Hess, K Horie, Richard G Jones, P Kratochvíl, I Meisel, I Mita, G Moad, et al. Definitions of terms relating to the structure and processing of sols, gels, networks, and inorganic-organic hybrid materials (iupac recommendations 2007). *Pure and Applied Chemistry*, 79(10):1801–1829, 2007.

[54] Jaime A Rincón Cardona and Cristián Huck Iriart. Confocal laser scanning microscopy (clsm) in foods. *Confocal Laser Microscopy: Principles and Applications in Medicine, Biology, and the Food Sciences*, page 203, 2013.

A Modifications in recipes

Modifications to improve the chosen recipes from literature was done and are described in appendix A.

A.1 Emulsion gel

The original recipe was adapted due to differences in protein purity between the source used in literature and the PPI available for this study. The original formulation used PPI with a protein content of 96.14% (calculated using a nitrogen-protein conversion factor of 5.96), and the PPI in this study had a protein content of 66.70% (conversion factor 5.4).

To compensate, the amount of PPI was adjusted to ensure the same amount of effective protein. The following equations were used:

$$\text{Effective nitrogen content (original)} = \frac{96.14}{5.96} = 16.13\%$$

$$\text{Effective nitrogen content (used)} = \frac{66.70}{5.4} = 12.35\%$$

$$\text{Nitrogen in 7.2 g of original PPI} = 7.2 \times 0.1613 = 1.161 \text{ g}$$

$$\text{Required PPI} = \frac{1.161}{0.1235} = 9.4 \text{ g}$$

However, even after adjusting for protein content, the emulsion gel did not gel as expected. This may be due to differences in the functional properties of the protein, such as source variability or age. To improve gelation, 2 wt% agar was added.

A.2 Bigel

Two key adjustments were made during the preparation of the bigel system:

- The stirring speed during hydrogel and oleogel formation was reduced from the original 1000 rpm to 200 rpm due to equipment limitations.

- In the original study, the homogenization of the bigel was performed at 3000 rpm for 2 minutes followed by 6000 rpm for 3 minutes. However, during preliminary tests, this was found to be insufficient to form a stable bigel. Therefore, the mixing was adjusted to 15000 rpm for 2 minutes, which was successful.

These adaptations were necessary due to limitations in the available lab equipment. With these changes, a stable bigel was produced.

B Gel test

To evaluate the gel-forming capability of the emulsion gel and bigel, a gel test was performed. The samples were transferred into glass vials and put in the refrigerator at 4°C overnight. The evaluation was performed the next day by inverting the vials to observe whether the material maintained its structure or flowed.

Both gels retained their shape without flowing, indicating successful gelation and sufficient internal network strength.

(a) Emulsion gel **(b)** Bigel

Figure B.1: Geltest performed on (a) emulsion gel and (b) bigel.

C Printing temperature evaluation

Appendix C presents the results from studying the influence of printing temperature on 3DP on both gels.

Printing parameters

All samples were printed using a 1 mm nozzle. Four temperatures were tested: 30°C, 40°C, 50°C, and 60°C. These specific temperatures were chosen based on four points of interest observed in the temperature sweep test, see Figure 4.1e, where the bigel exhibited distinct changes in behaviour, shifting between more solid-like and fluid-like states. The aim was to assess how temperature influences the structural integrity of the printed objects.
The same printing parameters as in study 1 was used.

Observation during parameter tuning

During the initial extrusion trials, an unintended observation was made. When attempting to extrude the emulsion gel using a larger nozzle diameter or at faster speed, the material exhibited uncontrolled flow behaviour, see Figure C.1. While not part of the structured temperature evaluation, this observation informed the decision to reduce the printing temperature to 40°C in study 2.

Results

As observed in Figure C.2, the emulsion gel exhibited consistent printability across all temperatures, showing little variation in quality. In contrast, the bigel samples, see Figure C.3, revealed a clear dependency on temperature. At lower temperatures, the printed structures lacked definition, while increasing the temperature improved this. At 60°C, optimal quality was observed.

Figure C.1: Visual observation of bigel extruded at high speed. Due to the rapid extrusion, the material was deposited in a more liquid-like state, forming uneven "pools" that quickly solidified upon deposition.

Conclusion

The evaluation confirms the results from the temperature sweep. The emulsion gel is not affected by temperature variations during printing, maintaining good shape throughout the tested temperature range. The bigel, however, required increased temperatures for optimal print quality, where 60°C was the optimal temperature for stable extrusion and structural integrity.

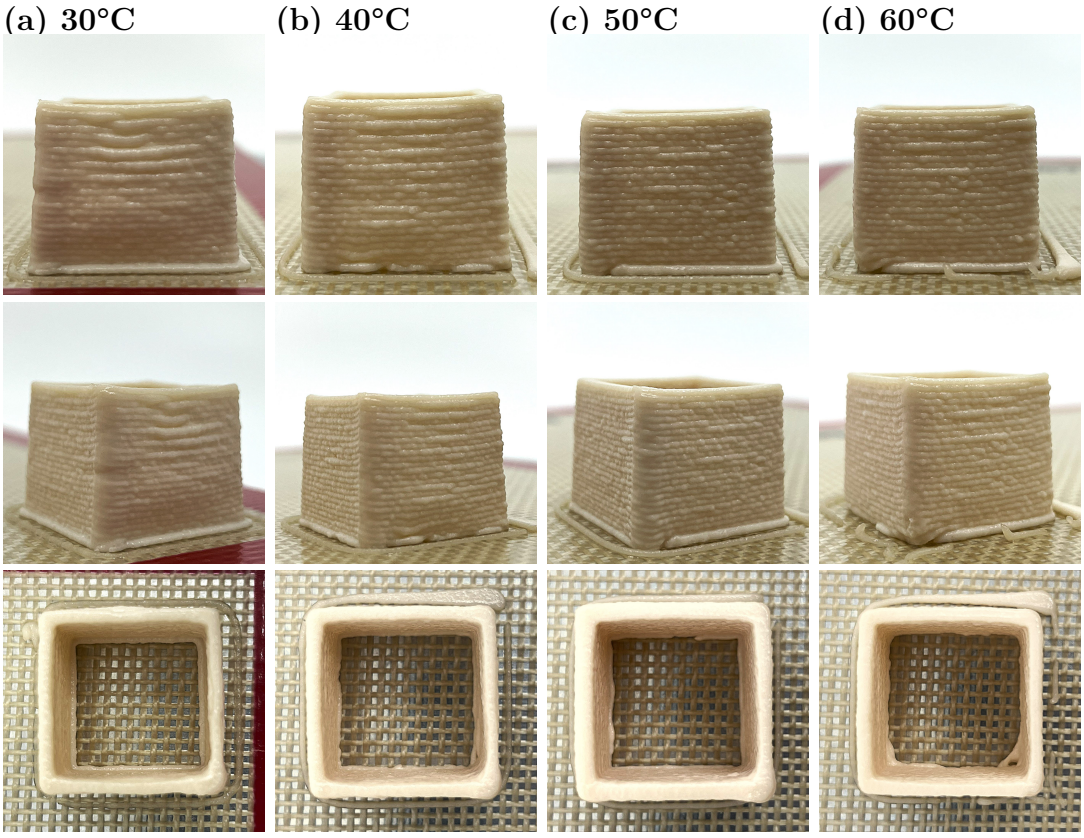

Figure C.2: Printed objects of emulsion gel at four different temperatures, (a) 30°C, (b) 40°C, (c) 50°C, and (d) 60°C. Each temperature is shown from the front, side, and top view. The images demonstrate how the printing temperature affects the structural integrity of the printed objects.

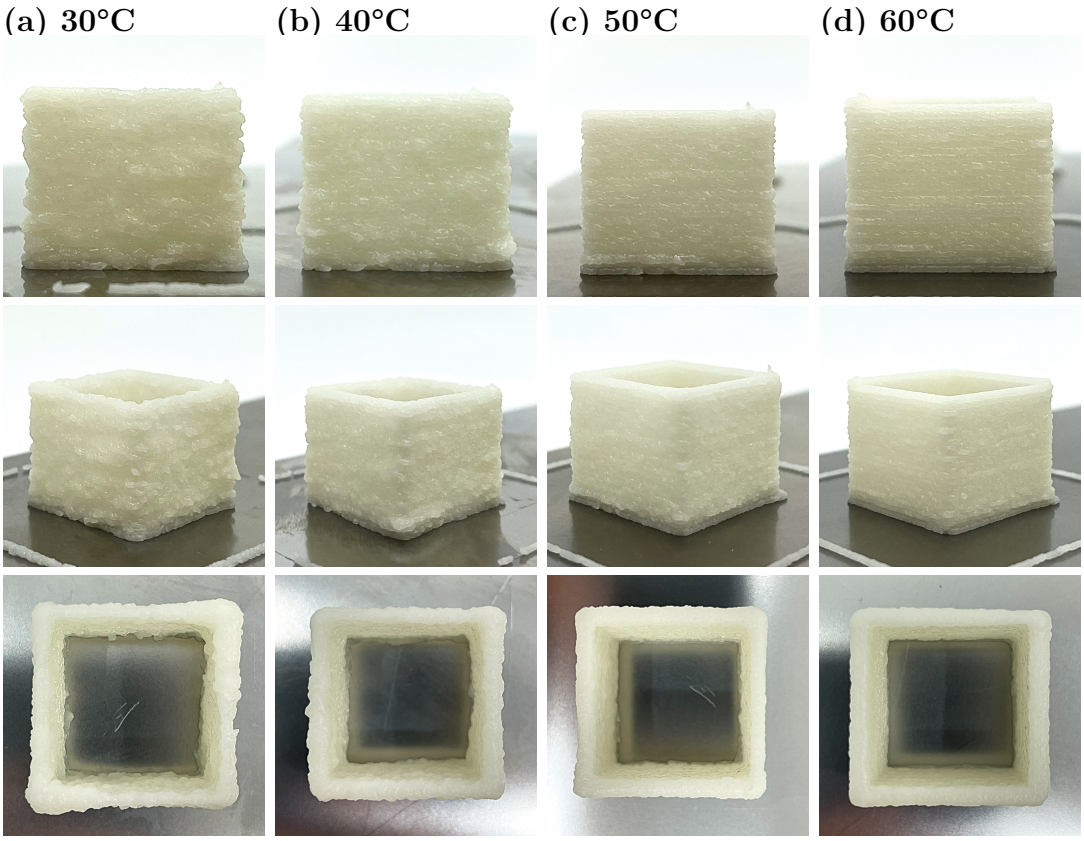

Figure C.3: Printed objects of bigel at four different temperatures, (a) 30°C, (b) 40°C, (c) 50°C, and (d) 60°C. Each temperature is shown from the front, side, and top view. The images demonstrate how the printing temperature affects the structural integrity of the printed objects.

D Further observations

D.1 Increased layer height

In a pre-study, increased layer height was tested during 3DP to assess the buildability and self-supporting capacity of the gels. The results are shown in Figure D.1.

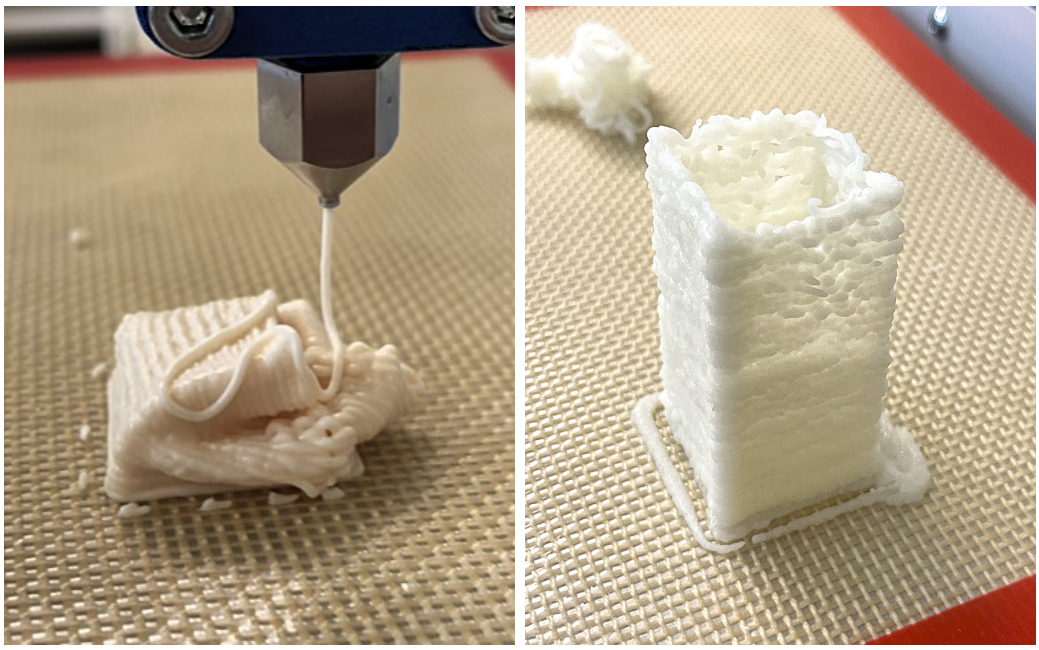

(a) Emulsion gel **(b)** Bigel

Figure D.1: 3D printing evaluating increased layer height as a part of a pre-study to evaluate the buildability of the gels. (a) Emulsion gel and (b) bigel.

While the bigel was capable of being printed at increased layer heights, it showed reduced resolution with the higher layers. However, it successfully supported the additional layers without collapsing. In contrast, the emulsion gel failed to maintain its structure under the same conditions and collapsed.

These findings highlight the superior structural integrity of the bigel compared to emulsion gel. Still, there is a need for optimization to improve definition throughout the printed object.

D.2 Self-supporting abilities of bigel

To further assess the self-supporting properties of the bigel, simple evaluations were conducted, involving positioning of the object and applying load. These tests aimed to explore the gel's ability to retain its form.

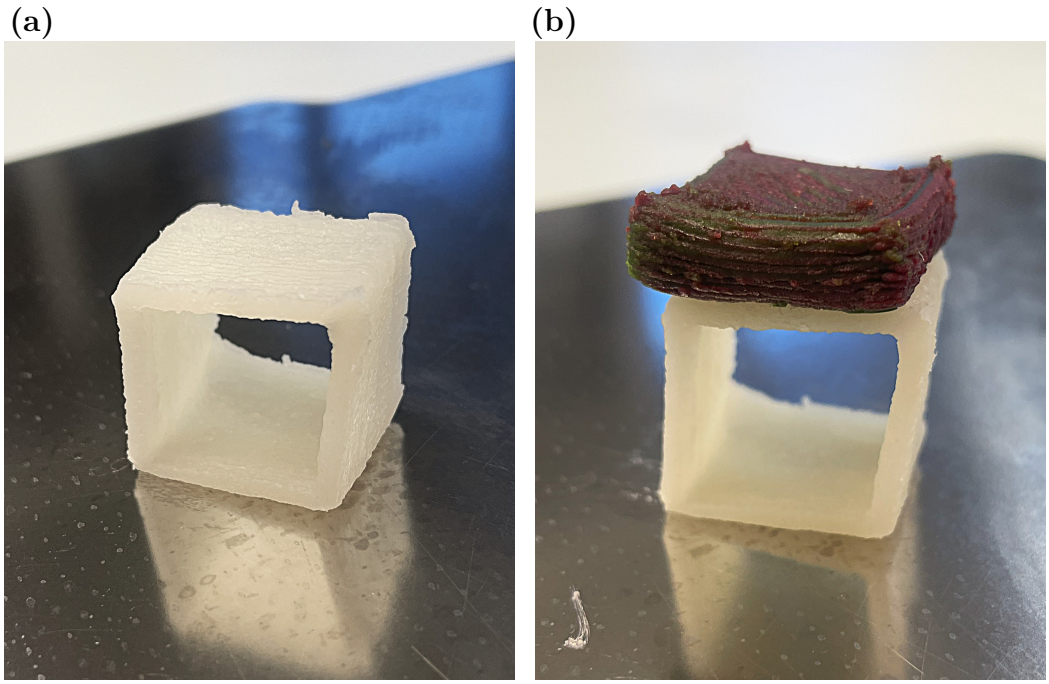

Figure D.2: Evaluation of bigel's structural integrity. (a) The printed object placed on its side to evaluate its ability to maintain shape without support, (b) A printed object of PPI30 was placed on top of the bigel structure to test its weight-supporting capacity. The bigel retained its form in both scenarios, demonstrating good self-supporting properties.

These observations confirmed that the bigel exhibited good stability. It maintained its shape both when put onto its side and when exposed to additional load, suggesting strong gel network, good structural integrity and favorable for 3DP applications.

D.3 Storage of emulsion gel

During the study, some printed samples of emulsion gel were unintentionally left at room temperature for 1–2 days, providing an opportunity to observe their storage stability.

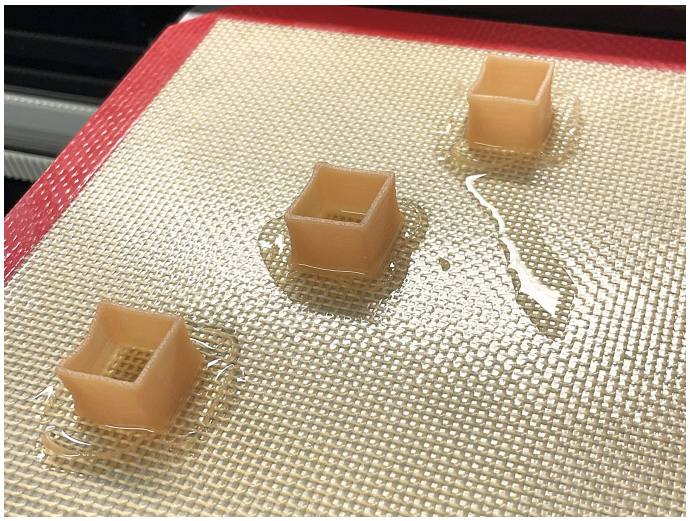

Figure D.3: Printed emulsion gel objects after being stored at room temperature. Liquid separation is visible around the samples, along with noticeable drying of the objects.

Figure D.3 shows visible signs of instability after the storage at room temperature. Water had evaporated, oil had leaked from the gel matrix, and a dry protein residue remained. This visual outcome illustrates the limited storage stability of the emulsion gel under ambient conditions.

In contrast, the bigel samples presented in Section D.2 maintained their structure even after more than a month at room temperature, with no visible leakage, phase separation, or surface deterioration, highlighting the superior long-term stability of the bigel formulation.

D.4 Leakage of emulsion gel during extrusion

During extrusion of the emulsion gel, an issue was occasionally observed where the material was not deposited through the nozzle as intended. This was particularly noticeable during MM3DP. Instead of being extruded from the nozzle together with PPI30, it came out at the connection point between the cartridge and the mixing module, shown in Figure D.4. This suggests that the emulsion gel sought "easier" pathways to exit the system, and highlights the need to further improve the rheological behaviour of the emulsion gel.

Figure D.4: Visual observation of leakage from the mixing module during extrusion of emulsion gel. The arrow indicates gel escaping at the cartridge connection point, suggesting that the material, due to its rheological properties, occasionally found alternative paths instead of exiting through the nozzle.

DEPARTMENT OF LIFE SCIENCES
CHALMERS UNIVERSITY OF TECHNOLOGY
Gothenburg, Sweden
www.chalmers.se

CHALMERS
UNIVERSITY OF TECHNOLOGY